Measurements of the Thermal Conductivity of Compressed Beryllium Pebble Beds

EFDA reference: TW2-TTBB-007a D4

J. Reimann, G. Piazza, Z. Xu, A. Goraieb, H. Harsch

**Institut für Kern- und Energietechnik
Programm Kernfusion**

Mai 2005

Measurements of the Thermal Conductivity of Compressed Beryllium Pebble Beds

EFDA reference: TW2-TTBB-007a D4

J. Reimann, G. Piazza, Z. Xu, A. Goraieb*, H. Harsch*

Institut für Kern- und Energietechnik

Programm Kernfusion

*Goraieb Versuchstechnik, Karlsruhe

Abstract

For helium cooled pebble bed blankets, the description of the thermal-mechanical interaction between pebble beds and structural material requires the knowledge of the pebble bed thermal conductivity k as a function of temperature T and deformation state (pebble bed strain ε).

In the frame of the EFDA Technology Work Programme TW2-TTBB-007a-D4, the measurements of thermal and mechanical parameters of beryllium pebble beds have been performed in the HECOP facility in the Forschungszentrum Karlsruhe. This report gives a summary of previous work on the thermal conductivity k of beryllium pebble beds, describes the experimental set-up, and presents the new experimental results.

The investigated pebble beds, consisting of 1mm pebbles, are representative for dense pebble beds (vibrated after filling, packing factors of $\approx$ 63.5%). Measurements were performed at bed temperatures between 200 and 650°C and maximum pebble bed deformations up to 3.5%.

For this parameter range, two different correlations for the thermal conductivity k as a function of pebble bed deformation ε and temperature T are proposed. The first one is primarily based on measurements but makes use of the conductivity values for non-deformed pebble beds predicted by the Schlünder Bauer Zehner (SBZ) model:

$$k(W/(mK)) = 1.81 + 0.0012\,T(°C) - 5\ 10^{-7}\,T(°C)^2 + (9.03 - 1.386\ 10^{-3}\,T(°C)$$
$$- 7.6\ 10^{-6}\,T(°C)^2 + 2.1\ 10^{-9}\,T(°C)^3)\ \varepsilon(\%). \tag{1}$$

It is expected that this correlation predicts also satisfactory values for beryllium pebble beds with pebble diameters different from 1mm and other packing factors than 63.5% as long as densified pebble beds are considered.

The second correlation connects the a priori unknown contact surface ratio ρ_k^2 of the SBZ model with the pebble bed deformation:

$$\rho_k^2(1) = 0.0041\ \varepsilon(\%) + 0.0021\ \varepsilon(\%)^2 \tag{2}$$

In combination with this correlation, the SBZ model can be also applied for compacted pebble beds consisting of other materials than beryllium.

Finally, another type of correlation is presented to be used if it shows that swelling due to irradiation effects results in much larger pebble bed deformations than mentioned above.

With the present data on beryllium pebble bed thermal conductivity, the corresponding data on thermal creep, also obtained in the HECOP facility, and the already existing data for ceramic breeder pebble beds, a complete set of pebble bed data exists now, relevant for the begin of reactor life where irradiation effects are still negligible. Now, calculations of the thermal-mechanical interaction between the pebble beds and the blanket structure in blanket relevant components could be started.

Messungen der thermischen Leitfähigkeit von komprimierten Beryllium-Schüttbetten

Zusammenfassung

Die Beschreibung der thermomechanischen Wechselwirkung zwischen Schüttbetten und Strukturmaterial in heliumgekühlten Pebble-Bed Blankets erfordert die Kenntnis der thermischen Leitfähigkeit k der Schüttbetten als Funktion der Temperatur T und der Schüttbett-Verformung (Dehnung ε).
Im Rahmen des EFDA Technology Work Programme TW2-TTBB-007a D4 wurden in der HECOP-Versuchseinrichtung des Forschungszentrums Karlsruhe Messungen der thermischen und mechanischen Eigenschaften von Beryllium-Schüttbetten durchgeführt. Dieser Bericht gibt einen Überblick über frühere Arbeiten über die thermische Leitfähigkeit von Beryllium-Schüttbetten, beschreibt den experimentellen Versuchsaufbau und stellt die neuen Ergebnisse vor.

Die Schüttbetten bestehen aus 1mm Kügelchen und sind repräsentativ für dichte Schüttbetten (nach Einfüllen vibriert; Füllgrade $\approx$ 63.5%). Die Messungen wurden in einem Temperaturbereich von 200 bis 650°C und maximalen Schüttbett-Verformungen bis $\approx$ 3,5% durchgeführt.

Für diesen Parameterbereich werden zwei verschiedene Korrelationen für die thermische Leitfähigkeit k als Funktion der Schüttbett-Deformation und -Temperatur vorgeschlagen. Die erste basiert im wesentlichen auf Messungen unter Benutzung des Leitfähigkeitswertes für undeformierte Schüttbetten gemäß dem Schlünder Bauer Zehner (SBZ) Modell:

$$k(W/(mK)) = 1.81 + 0.0012\,T(°C) - 5\cdot10^{-7}\,T(°C)^2 + (9.03 - 1.386\cdot10^{-3}\,T(°C)$$
$$- 7.6\cdot10^{-6}\,T(°C)^2 + 2.1\cdot10^{-9}\,T(°C)^3)\,\varepsilon(\%). \qquad (1)$$

Es wird erwartet, dass diese Korrelation auch zufriedenstellende Werte ergeben sollte für Beryllium-Schüttbetten mit anderen Pebble Durchmessern und Füllgraden als 1mm bzw. 63.5%, solange dichte Schüttungen vorliegen.

Die zweite Korrelation verknüpft das a priori unbekannte Kontaktflächenverhältnis ρ_k^2 des SBZ Modells mit der Schüttbett-Deformation:

$$\rho_k^2(1) = 0.0041\,\varepsilon(\%) + 0.0021\,\varepsilon(\%)^2 \qquad (2)$$

In Kombination mit dieser Korrelation kann das SBZ Modell auch für kompaktierte Schüttbetten angewandt werden, die aus anderen Materialien als Beryllium bestehen.

Schließlich wurde noch ein Typ von Beziehungen angegeben, für den Fall dass Schwellen von Beryllium aufgrund von Bestrahlungseffekten sehr viel größere Schüttbett-Deformationen bewirkt als oben aufgeführt.

Mit den jetzt zur Verfügung stehenden Daten über thermische Leitfähigkeit von Beryllium-Schüttbetten, den entsprechenden Daten zum thermischen Kriechen, die ebenfalls in der HECOP-Anlage gewonnen wurden und den bereits bestehenden Daten für keramische Brutmaterial-Schüttbetten liegt ein vollständiger Datensatz vor, relevant für den Beginn des Reaktorbetriebs, für den Bestrahlungseffekte noch vernachlässigbar sind.

Mit diesen Daten kann jetzt die Beschreibung der thermomechanischen Wechselwirkung zwischen Schüttbetten und Strukturmaterial in blanketrelevanten Komponenten in Angriff genommen werden.

Contents

1. INTRODUCTION

In the helium cooled pebble bed (HCPB) blanket for fusion power reactors the neutron multiplier and the breeder material are arranged in pebble beds between flat cooling plates [1]. The maximum temperatures in the breeder and beryllium pebble beds are about 900 °C and 650 °C, respectively. Temperature differences and different thermal expansion coefficients between pebble beds and structural materials as well as irradiation effects (swelling of the beryllium up to 10 volume % during the blanket lifetime has been assessed) cause constrained strains, which imply elastic and plastic deformations in the pebble beds. These deformations influence the effective thermal conductivity of pebble beds, especially for beryllium pebbles in helium atmosphere because of the large ratio of beryllium conductivity to gas conductivity. For ceramic breeder pebble beds, this ratio is much smaller and with this the influence of deformation [2].

The modelling of the thermal-mechanical interaction between pebble beds and structural material behaviour requires, therefore, as important input data the dependence of the thermal conductivity of beryllium pebble beds as a function of temperature and deformation state. Although the deformations are caused by stresses imposed on the pebbles, the stress is not a useful quantity because there is no unique relationship between stress and strain: at elevated temperatures thermal creep occurs and, therefore, different deformation states may correspond to the same stress values. In this report, the bed deformation, characterised by the bed strain ε, is considered as prime parameter and the dependence of the thermal conductivity k on strain ε and temperature T is investigated.

There are results from several investigations on the thermal conductivity of beryllium pebble beds. However, most of them are related to non-deformed beds, see e. g. [3-5]. Only in a few investigations, a pressure was imposed, but mostly without measurement of bed strain, compare e.g. [6, 4, 7]. There is only one reference [8] with results on strongly deformed pebble beds where both pressure and pebble bed strain were measured.

The experimental set-ups used in the above mentioned investigations are essentially of two types, as shown schematically in Fig.1.1:

a) axis-symmetric bed arrangements, where the heat flux generated in a central heater rod is radially transferred through an annular pebble bed to an outer cooled cylindrical shell;

b) uniaxial arrangements, where cylindrical pebble beds are compressed in the direction of the cylinder axis (uniaxial compression) with a heat flux in the same direction (e. g. heated bottom plate, cooled piston).

The essential advantage of the axis-symmetric arrangement is that heat losses are of negligible concern if the axial bed length is large compared to the bed diameter. On the other hand, bed deformations can be neither imposed in a controlled manner nor measured. This arrangement is well suited for investigations of non-deformed pebble beds [3, 4, 5], although attempts were also made to generate deformations by using large temperature differences in the bed [4].

The uniaxial set-up [6-8] offers the possibility to vary and measure independently temperature, bed pressure (uniaxial stress), and bed deformation (uniaxial strain). The main disadvantage of uniaxial arrangements is that heat losses in radial or axial directions are difficult to control. Great attention has to be paid on the measurement of these heat losses in order to obtain accurate experiments.

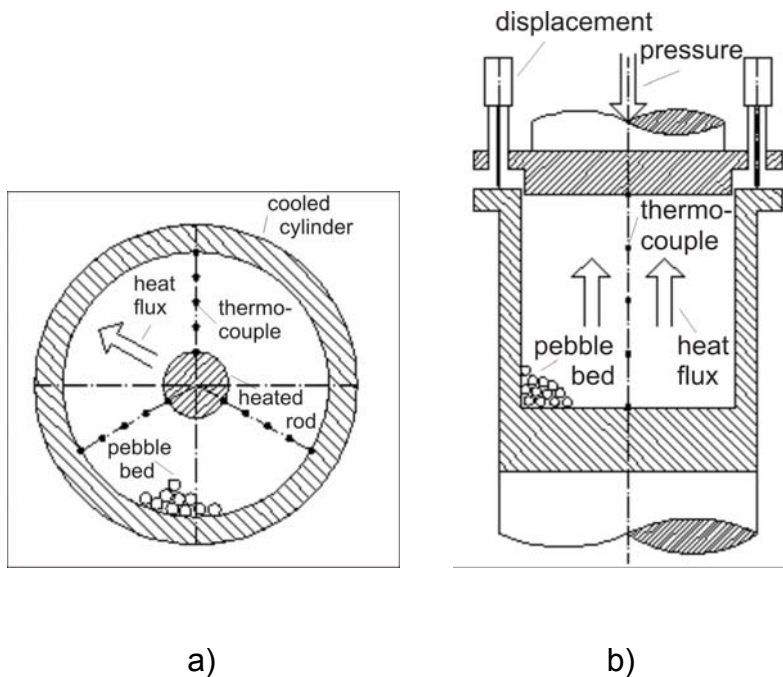a)   b)

Fig. 1.1. Experimental set-ups used for pebble bed conductivity measurements

Another problem using uniaxial set-ups for measurements with non-deformed (non-compressed) pebble beds is the following: in order to have a defined heat flux, a minimum piston pressure is required. For temperatures above ≈ 400°C, thermal creep [9] might be caused already by such small bed pressures resulting in non-negligible pebble bed deformations. If deformations are not measured, they cannot be controlled.

For the two arrangements discussed above, heating rods or plates were mentioned which are operated in steady-state condition. An attractive alternative to this is, because of its simplicity, the "Hot Wire Technique" (HWT) where a thin wire, embedded in the pebble bed, is heated up instantaneously and the surface of the wire is measured as a function of time. This technique was used first by [3] for the investigation of thermal conductivity of non-deformed ceramic breeder and beryllium pebble beds and was combined by [8, 10] with an uniaxial compression test set-up for investigations of strongly deformed ceramic breeder and beryllium pebble beds.

The HWT is a standard technique for low conductivity materials but the accuracy for materials like beryllium is somewhat questionable. Therefore, in order to perform measurements with a higher accuracy and covering a larger parameter range, the test facility HECOP, belonging to type b) equipments, was built. Details are outlined in Section 3. In Section 4, new results obtained with a modified version of HECOP will be presented. Already published results [11] obtained with the older version will be presented in Section 2.

## 2. SUMMARY OF PREVIOUS RESULTS

2.1 Non-deformed pebble beds

The knowledge of the thermal conductivity of pebble beds is of interest in many engineering areas, and different models exist in literature to predict k as a function of the relevant parameters. These models are based on idealised pebble arrangements; however, the main parameters of influence are taken mostly into account. The Schlünder-Bauer Zehner (SBZ) model is one of the options, frequently used for

comparisons with experimental data. Attention has to be paid on the fact that different model versions exist: in the versions published before 1994, see e.g.[12], either no value for the accommodation factor for helium was given or a constant value of 0.4; whereas in the later versions, compare e.g. [13], this factor is dependent on temperature and has for blanket relevant temperatures a value of ≈ 0.22. This modification results in conductivity values for non-deformed beds which are lower by about 15% compared to the older model versions. With increasing compaction, the differences become smaller. In this report, the new version of the SBZ model [13] will be used.

The SBZ contains as important parameter the quantity ρ_k^2 which is the ratio of contact area between two adjacent pebbles related to the projected area of the pebble, $\rho_k^2 = (d_c/d)^2$, (d_c and d are the contact area and pebble diameter, respectively). This parameter is a priori not known and must be correlated with measurable pebble bed quantities.

In the following, a brief summary of previous experimental results for beryllium pebble beds is presented, without claiming completeness. First, results for non-deformed pebble beds are discussed. Figure 2.1 presents the thermal conductivity as a function of temperature for beds consisting of 2mm diameter pebbles: In Fig. 2.1a results from [4] for a packing factor of 63% are presented; in Fig. 2.1b results from [7] and a comparison with other authors [3, 4]. In Fig.2.2 some of these data are compared with predictions of the SBZ. The pebble bed conductivity is expected to increase with temperature T, because the helium conductivity increases with T. This effect is clearly seen in all data. The temperature effect predicted by the SBZ, however, is significantly smaller than found in the measurements. As mentioned above, it is difficult to ensure that with increasing mean bed temperatures, pebble deformations can be avoided, especially if an uniaxial set-up is used. An example for this are the experiments [7] where the highest mean temperature was 420°C with temperature differences across the bed of ≈ 400°C, thus maximum bed temperatures above 600°C. For axis-symmetric set-ups, the possibility of pebble deformations might be smaller, as outlined before, but it can not be totally excluded.

For non-deformed beds, $\rho_k{}^2 = 0$ should be the relevant value in the SBZ model. However, it is generally observed that for this value the SBZ model predicts a too small conductivity. Contact surfaces larger than zero might already exist for non-compressed pebble beds because of e.g. surface roughness or some internal stress build-up during filling, often performed with vibration. Therefore, $\rho_k{}^2$ values of slightly larger than 0 are recommended [13]; for beryllium pebble beds, $\rho_k{}^2 = 10^{-4}$ was proposed by [3]. Figure 2.2 contains the influence of this parameter: for blanket relevant temperatures (350< T(°C) <750). The conductivity values are shifted upwards by about 10% which is a relatively small change compared with the strong influence of deformation, discussed in Section 2.2.
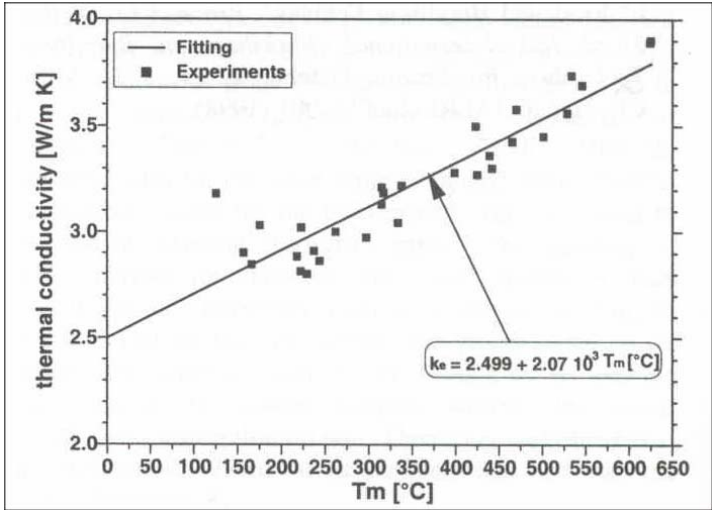
a)   Results from [4], packing factor 63%.
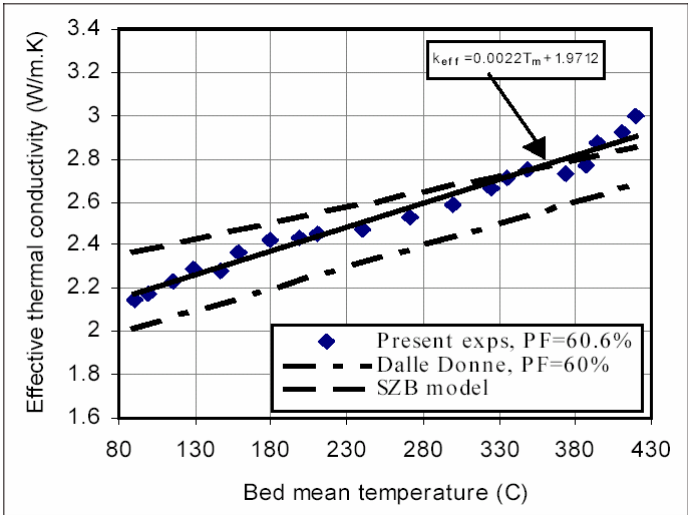
b)   Results from [7]

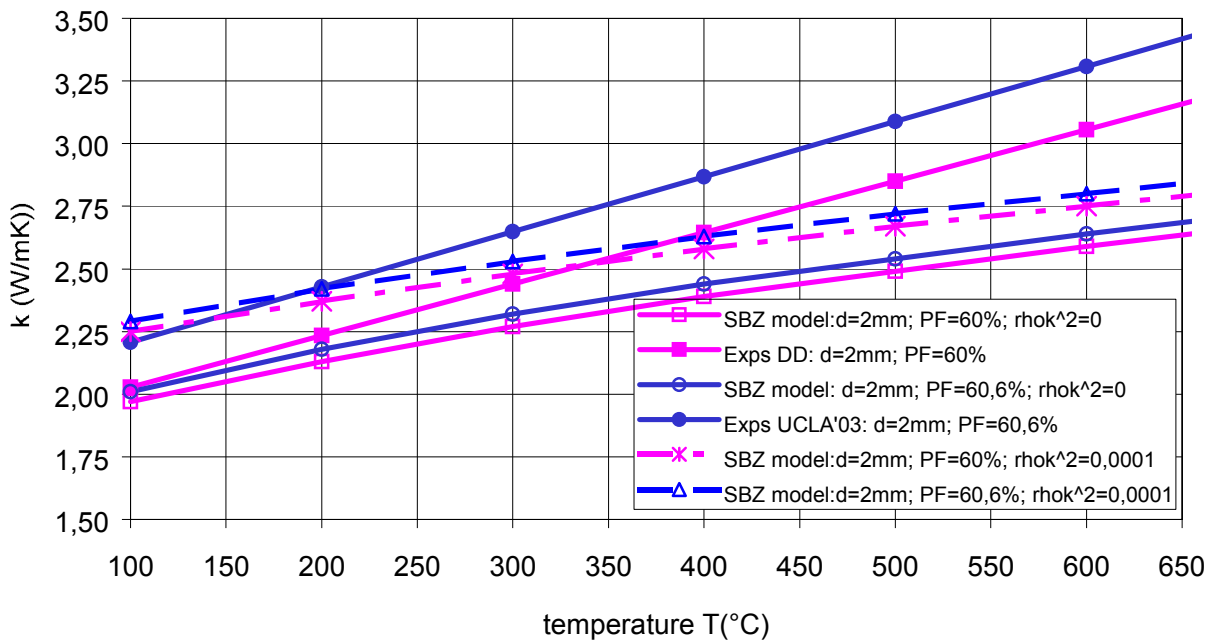Fig. 2.1 Thermal conductivity of non-deformed beryllium pebble beds.
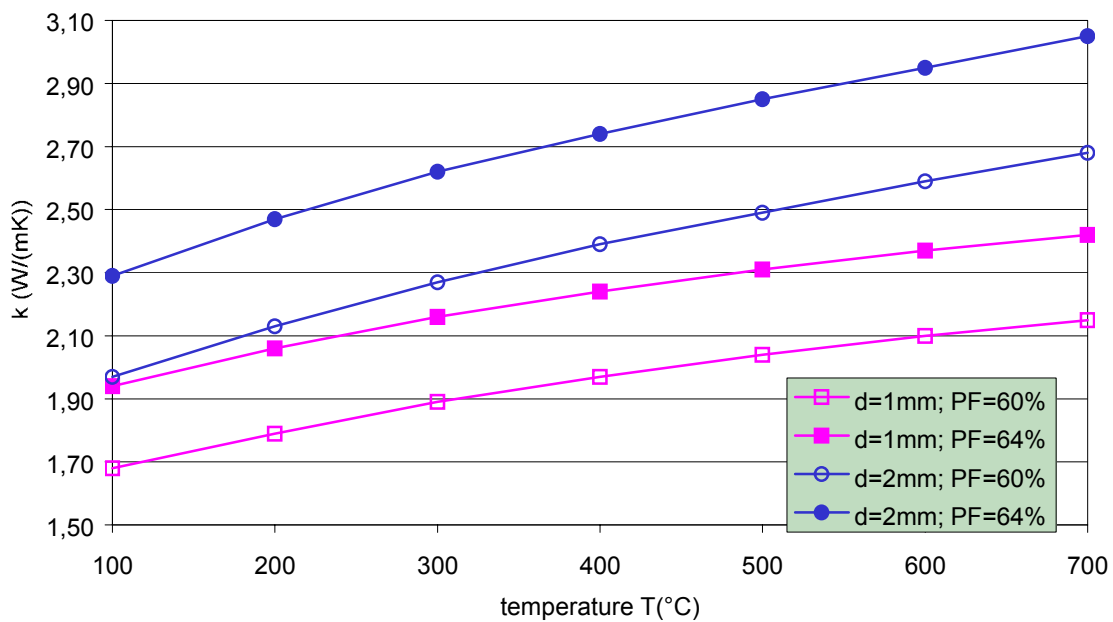
Fig. 2.2. Comparison of results with SBZ model.

Fig. 2.3. Influence of d and   for non-deformed beds (SBZ).

Experimental data exist for different pebble diameters d and packing factors γ (ratio of volume covered by beryllium to total volume). Figure 2.3 again shows SBZ predictions for different values: The thermal conductivity increases both with

6

increasing d and increasing γ; for the given values the differences are again so small that it is difficult to quantify these effects experimentally.

A critical comment should be made in respect to packing factor γ: it has been known for long [14] that the maximum packing factor, achieved for beds densified by vibration, increases with the ratio of container diameter D to pebble diameter d and reaches a constant value for D/d > 100. The ultimate value depends on pebble shape, pebble surface and size distribution; for mono-sized spheres values of about 63% were reported [14]; different diameters and deviations from sphericity can increase this value.

The reason for decreasing packing factors with decreasing container dimensions is the increasing influence of container walls: the packing factor close to walls is significantly smaller than in the bulk. Therefore, the global packing factors obtained for experimental set-ups might not always be relevant for the bulk packing factor existing in these set-ups, for which the thermal conductivity is determined. Another point is that internal components like thermocouple rakes represent also local disturbances that could decrease the global packing factor.
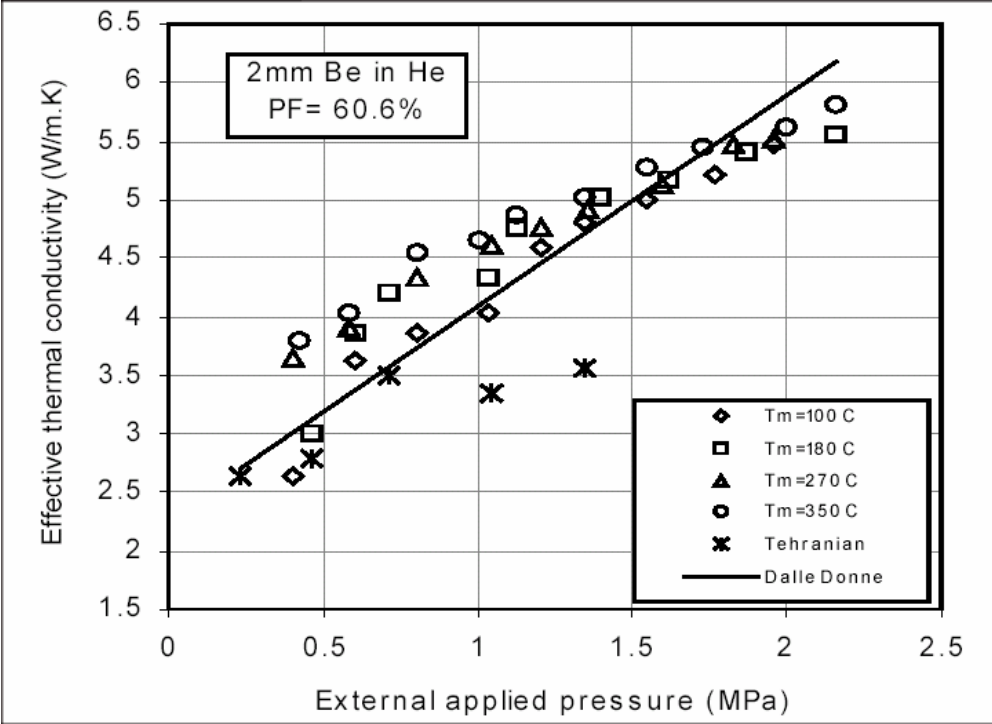

Fig. 2.4. Results from [7]: k=f(p).

2.2 Deformed pebble beds

Figure 2.4 shows data from experiments from [7] for deformed pebble beds where the pressure was measured but not the bed strain. The data from [6], put in the same plot, are the lowest; the data from [4] agree with those from [6] at low pressures but are much higher at large values; a linear dependence between k and p was observed. The results from [7] are the largest at low pressures and are characterised by a smaller pressure dependence than those of [DanneDonne1].

Figures 2.5-2.8 contain results from the first experiments with deformed pebble beds where besides the external pressure the bed deformation was also measured [8]. As mentioned before, the HWT was used in these experiments. Figure 2.5 shows the stress-strain dependence and thermal conductivity of pebble beds (packing factors $\gamma \approx 63\%$) consisting of 1mm NGK beryllium pebbles at T=485°C: a strong increase of k with p is observed. The stress-strain curve indicates clearly at which pressure levels the HW measurements were performed: there is a small thermal creep strain period. This period is very small because HW measurements are performed in time periods of less than half a minute, in contrast to stationary measurements where time periods in the order of hours is required to reach quasi steady-state conditions.
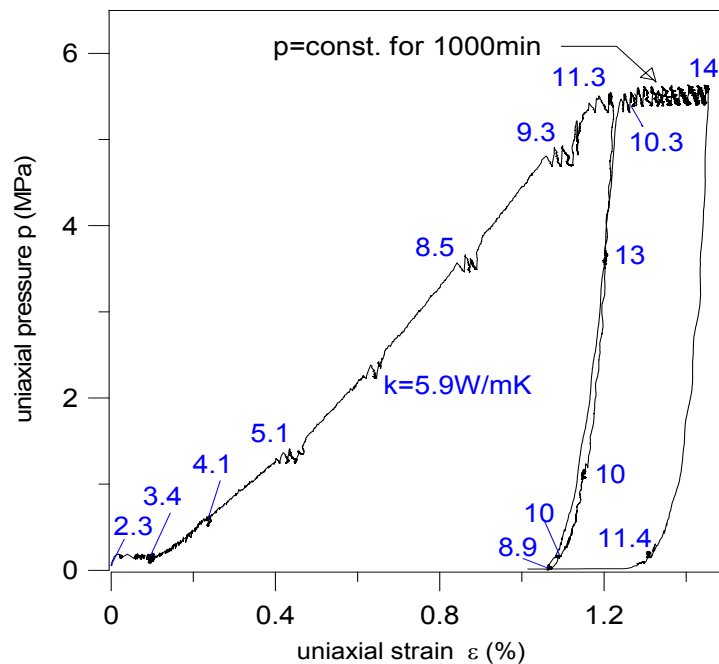

Fig.2.5. Stress-strain dependence for T = 485°C and measured conductivities ([8]).

8

Figure 2.5 also shows the dependence of thermal conductivity during the pressure decrease period: because of primarily plastic pebble deformations, the bed strain does not vary significantly during pressure decrease, nor does the thermal conductivity, except at very low pressure levels where contact surfaces are expected to detach.
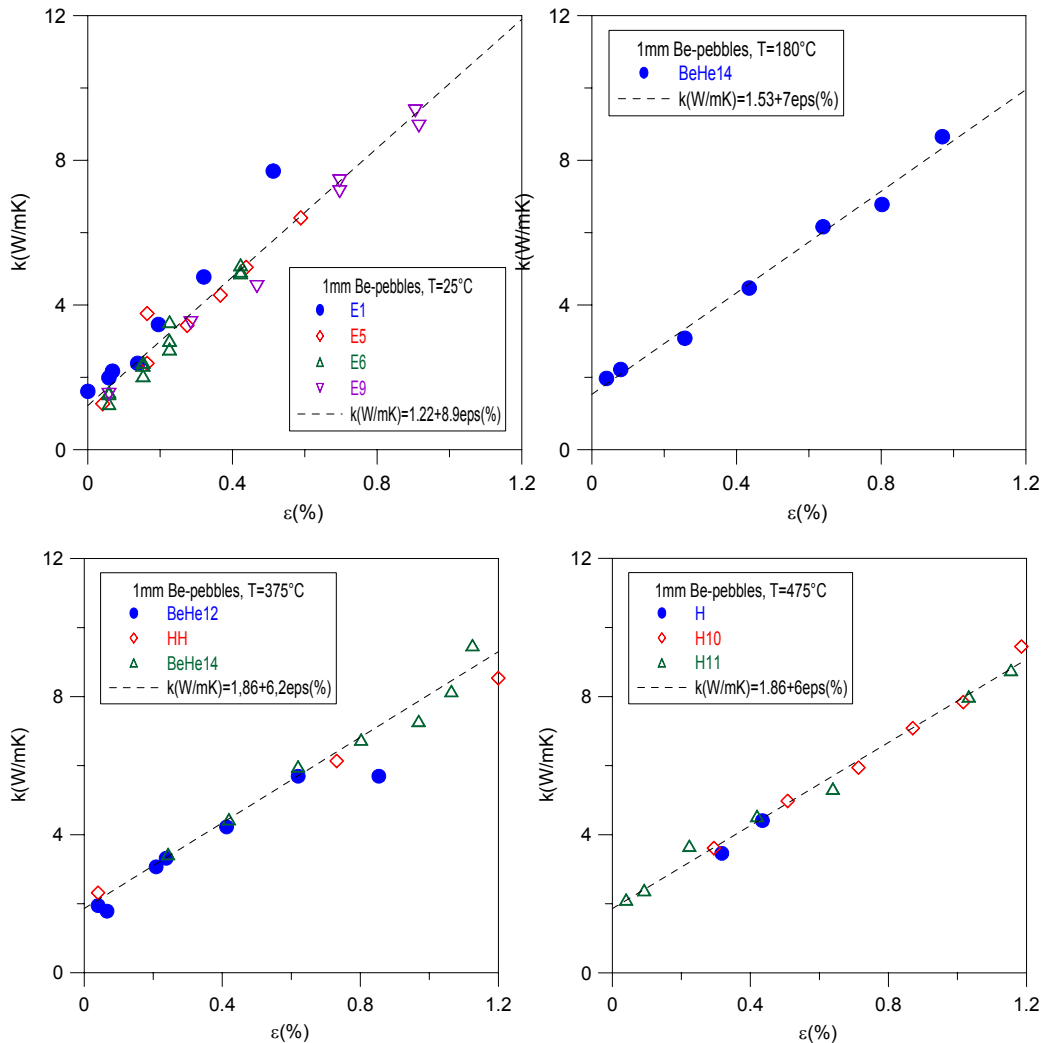

Fig.2.6. Thermal conductivity as a function of strain (1mm pebble beds) ([8]).

Figure 2.6 shows the thermal conductivity of 1mm beryllium pebble beds at different temperatures as a function of uniaxial bed strain ε. An important result is the well expressed linear dependence between k and ε. With increasing temperature, the slope should become smaller due to the decrease of beryllium conductivity with increasing temperature. This effect is most clearly seen in Fig. 2.7, where a normalised conductivity k* is used, defined as k* = $(k-k_{SBZ})/k_{SBZ}$, where k_{SBZ} is the conductivity for non-deformed pebbles beds according to the SBZ model [13]. Then,
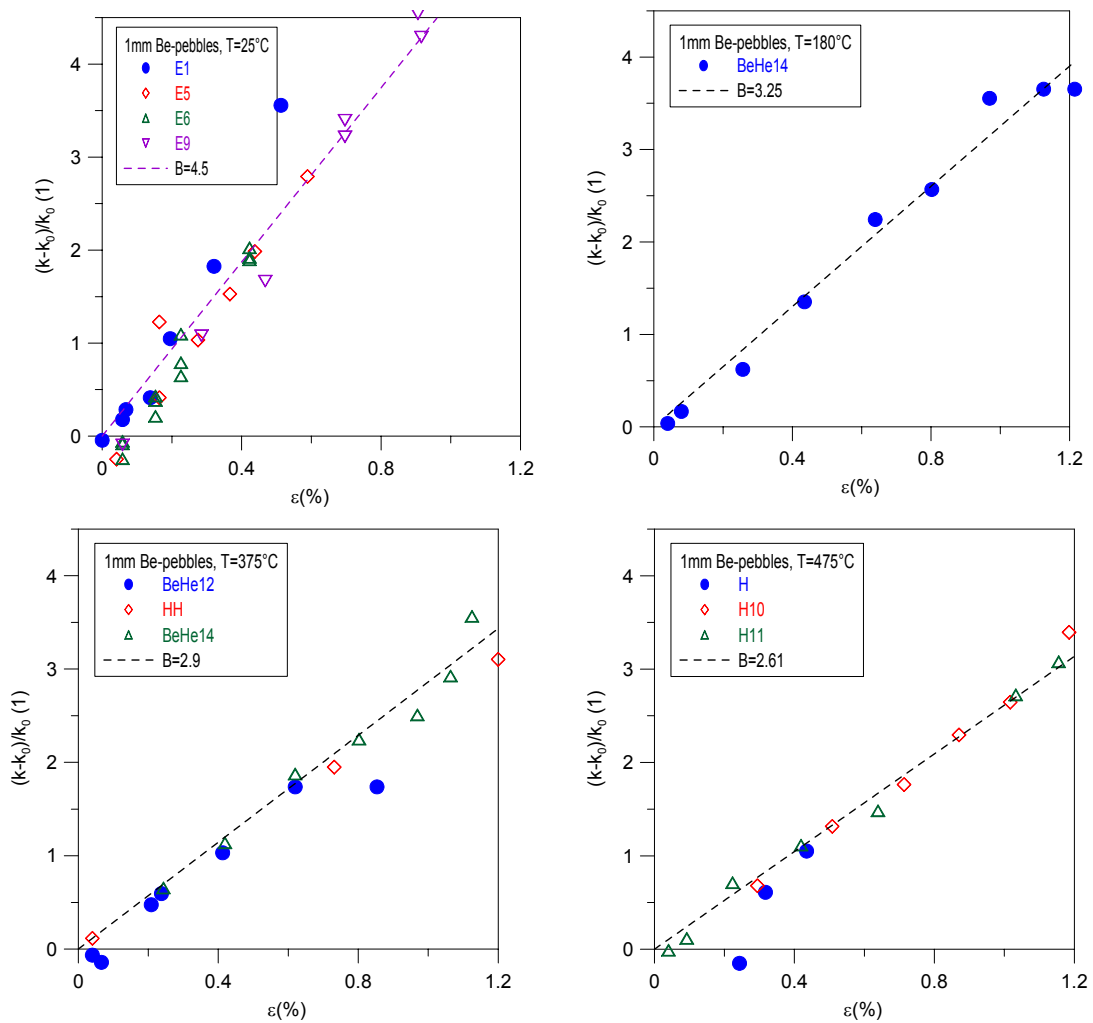
Fig.2.7. Normalised thermal conductivity as a function of strain (1mm pebble beds), ([8])

k* can be approximated well by k* = B(T)ε, and the values of B decrease with increasing temperature.

Figure 2.8 shows corresponding results for 2mm pebble beds: the conductivity is slightly higher than for 1mm pebbles; again the linear dependence is well pronounced.

Figure 2.9 shows a characteristic result from the first HECOP experiments [11], covering a strain range of about 1%: Again the non-linear dependence of k from p is observed and a rather linear dependence of k on bed strain ε. Compared to the HWT results, the conductivity values are larger by about 25%.

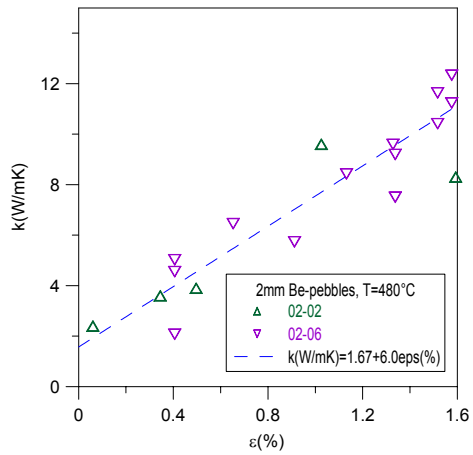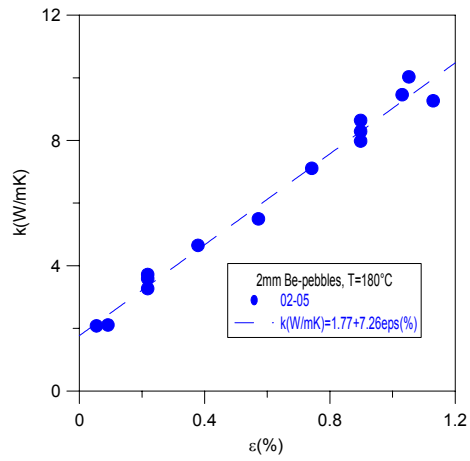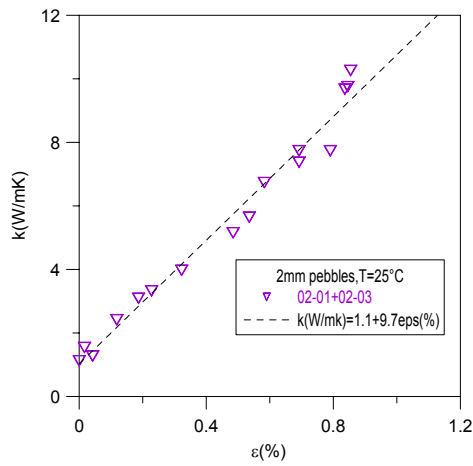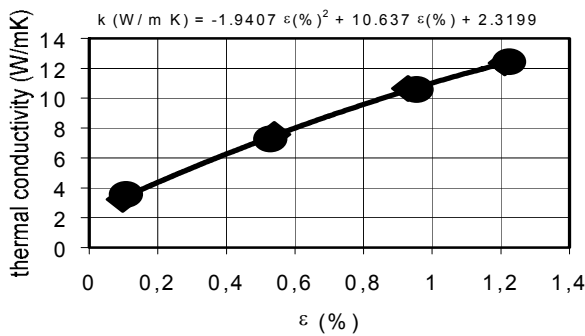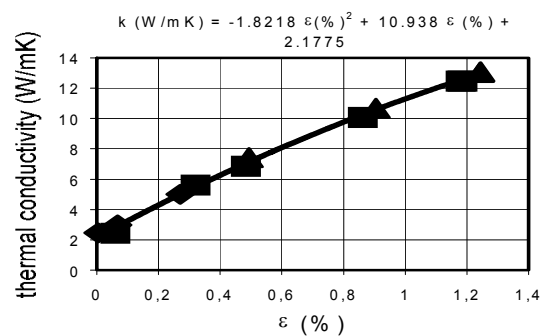Fig.2.8. Thermal conductivity as a function of strain (2 mm pebble beds), ([8])

a)T=250°C

b)T=350°C

Fig. 2.9. Thermal conductivity as a function of strain (HECOP I experiments with 1mm beryllium pebble beds ([11]).

Summarising previous data one can state that the amount of data for non-deformed beryllium pebble beds can be considered to be sufficient. In relation to deformed pebble beds, however, there are only two sources where deformation measurements were reported. These results differ by about 25% which is considered as a rather

11

large difference. Therefore, there is still a need for further tests, especially at higher temperatures and larger pebble bed deformations.

A critical comment is made concerning the use of uniaxial set-ups for heat conductivity measurements in comparison with the conditions which exists in the blanket. In uniaxial set-ups the heat flux is parallel to the uniaxial stress which is significantly larger than the stresses normal to this direction. Therefore, the question arises if the contact zones between pebbles are also larger in the direction of the uniaxial stress than in other directions. If this was the case, the pebble bed thermal conductivity would be non-isotropic with the largest value being measured by uniaxial experiments. In the blanket, the situation is much more complicated: heat is produced by internal heat sources that might imply that the pebble deformations are distributed homogeneously. However, the stresses due to constrained expansions are dependent on the temperature distribution in the pebble bed geometry and might be the largest in direction of the heat flux.

Microtomographic investigations on the topology of uniaxially deformed pebble beds were presented recently [15, 16]. Figure 2.10 shows the contact surface ratio A_c/A as a function of the poloidal angle δ (starting with 0 at the "North Pole"). For the non-compressed bed S0, about 70% of the data exhibit values of $A_c/A \approx 0.1\%$ which are interpreted as point contacts. The smaller group with $A_c/A \approx 2\%$ occurs probably because of the non-perfect sphericity of the pebbles. The bed deformation of sample S1 was $\varepsilon \approx 6\%$; that of sample S6 was $\varepsilon \approx 10.5\%$. With increasing pebble bed deformation, the group with $A_c/A \approx 0.1$ becomes smaller and the tendency becomes very pronounced that the contact surfaces increase preferentially in zones with $\delta < 45°$ and $\delta > 145°$, that is, in zones with large fractions of the contact surfaces normal to the uniaxial stress. These results confirm the concern that heat flux measurements in UCT set-ups could result in too high values. However, it is not possible yet to quantify this effect.
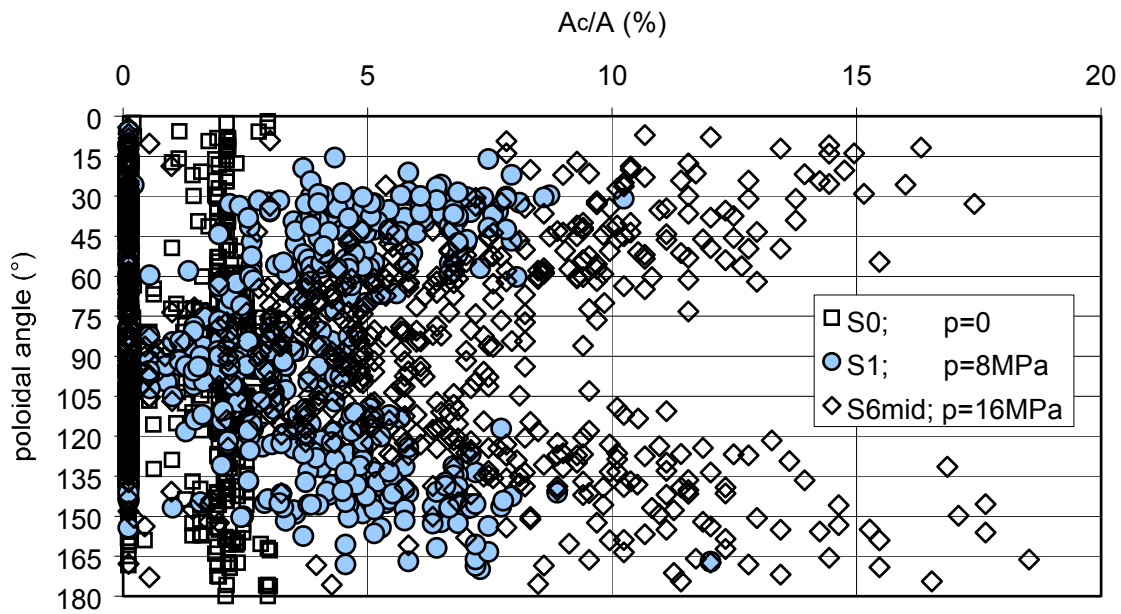
Figure 2.10. Angular distribution of contact surfaces for uniaxially deformed pebble beds (from [15]).

2.3 Highly deformed pebble beds (sintering processes)

Although bed deformations in blanket components might not exceed significantly 1% at beginning of live (BOL), swelling due to irradiation might result at the end of life (EOL) in deformations being larger by one order of magnitude. Therefore, there is interest for a correlation applicable for very high pebble bed compactions, even covering the situation that the final packing factor approaches 100%. The dependence of the thermal conductivity on bed deformation in this deformation range is of interest for sintering processes.

Figure 2.11 shows a graph from [17] where the ratio of the pebble bed conductivity, k_{eff}, to the conductivity of the solid material, k_s, is plotted as a function of the relative density which is identical with the packing factor γ with unit (1). In the figure, the initial packing factor is γ = 60% and the bed is compacted up to 100%. There is a reasonable agreement between measured data at large compactions and the following relationship:

$$k_{eff}/k_s = ((\rho-\rho_0)/(1-\rho_o))^{1.5\,(1-\rho_o)} , \quad (2.1)$$

where $(\rho-\rho_0)$ is equal to the bed deformation $\varepsilon(1)$ and $(1-\rho_o)$ is equal to the initial porosity which is $(1-\gamma(1))$.

However, it is obvious from Fig. 2.11 that Correlation (2.1) does not predict reasonable values for very small deformations that are important for fusion reactor blankets.
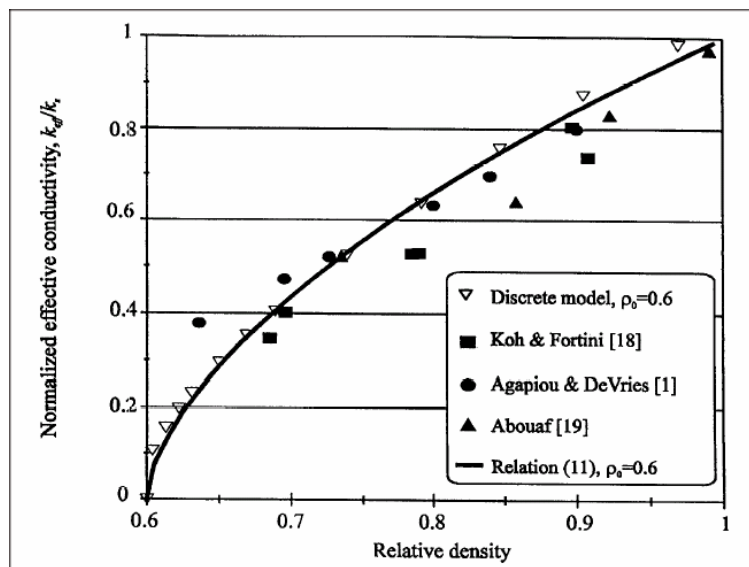

Fig. 2.11 Thermal conductivity of strongly densified pebble beds ([17]).

3. THE HECOP II FACILITY

3.1 Design description

The design requirements of HECOP (**HE**at **CO**nductivity in **P**ebble beds) were: independent adjustment of temperature and deformation of the beryllium beds, minimisation of uncontrolled heat losses, and reliable measurement of temperature gradients in the bed. Operating ranges were: maximum pressure p $\approx$ 6MPa; maximum average pebble bed temperature T $\approx$ 600°C. After the experiments at T = 250°C and 350°C, the experiments were terminated because of the failure of an

important component. It was decided not to replace this component but to redesign completely the facility and to build HECOP II. The characteristic features of the old version (HECOP I) in respect to the thermal control were not changed and corresponding electric components were used again.
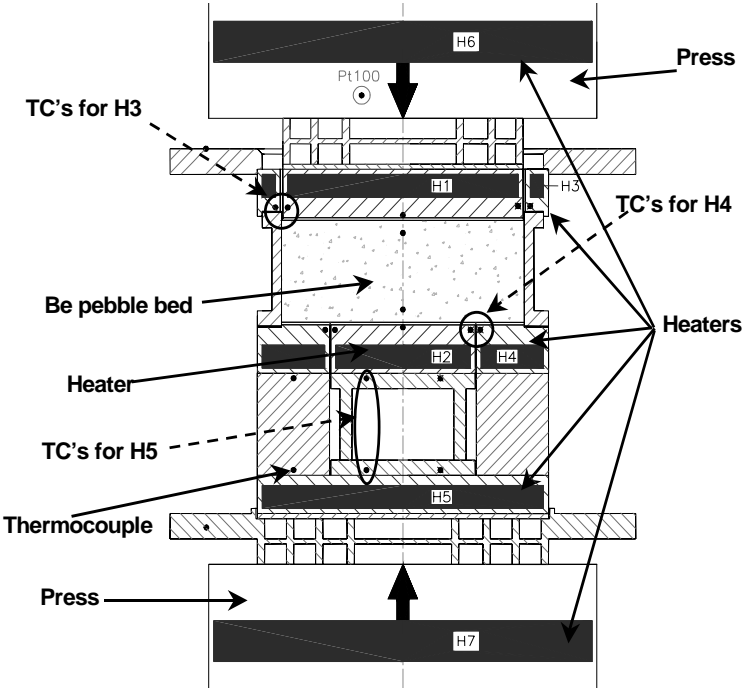
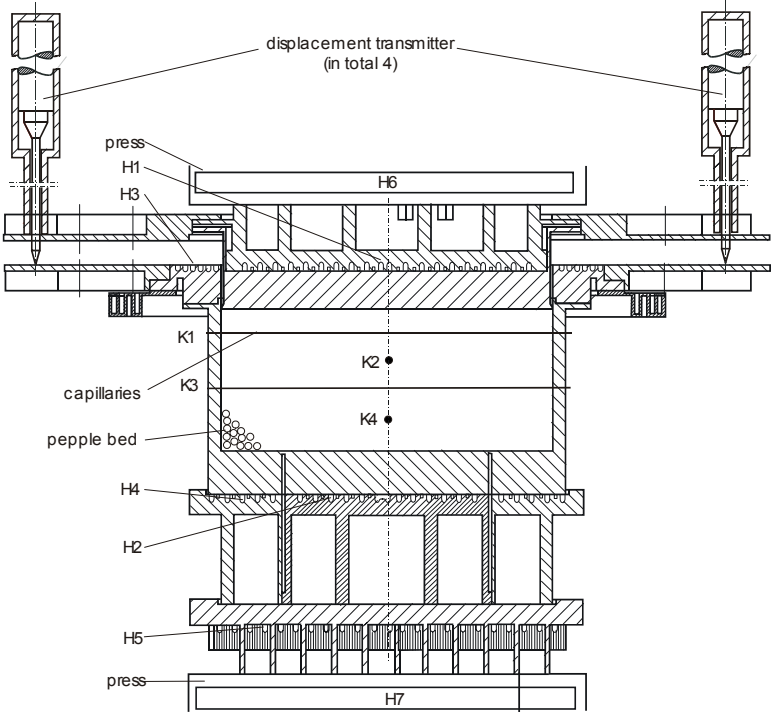

Fig.3.1. HECOP I test section

Fig. 3.2. HECOP II test section.

Figure 3.1 shows schematically HECOP I, and Fig. 3.2 contains a drawing of HECOP II. Both systems are positioned between the pistons of a hydraulic press (maximum load: 50 KN). For thermal control, a system of 7 heaters (H1-H7) is used. The desired temperature gradient in the pebble bed is produced at the bottom by the heaters H2 and H4 and at the top by the heaters H1 and H3.

H3 and H4 are guard heaters, which are used to minimise the radial heat losses by controlling the power such that the temperature difference between two neighbouring thermocouples becomes zero, (see Fig. 3.1).

H2 is used to calculate the thermal bed conductivity k by

$$k(W/(mK)) = (Q-Q_{loss}) \Delta x / \Delta T \qquad [3.1],$$

where Q [W/m^2] the heat flux produced by H2, Δx (m) the axial distance between the thermocouples in the bed and ΔT(K) the corresponding temperature differences. Q_{loss} is the residual heat loss which is determined by isothermal experiments, for details see Section 4.

In order to minimise the axial heat flow from H2 to the press bottom plate, the heater H5 is controlled such that the temperature difference of the thermocouple pair in H2 and H5 becomes zero.

In order to reach the highest bed temperatures, the heaters H6 and H7 that are part of the press are required.

The set-up is thermally insulated by refractory ceramic fibre (Kerlane) and was operated in the glove box with a helium atmosphere of 0.1MPa.

Compared to HECOP I, the essential modifications are the following:

1. pebble bed container with larger diameter and height with 4 capillaries (2mm outer diameter) at different bed heights where each contains 5 thermocouples at different radial directions,

2.   larger number of thermocouples (in total 60) in order to measure in more detail the temperature distribution in the total system,

3.   larger heating powers of heaters H2, H4, H5 in order to reach higher maximum temperatures. This is an important improvement because HECOP II is also used to measure thermal creep of beryllium beds,

4.   measurement of the bed displacement by measuring the displacement between piston and pebble bed container using two rings which are fixed on the piston and container, respectively. In HECOP I, the displacements were measured between the two rings above H1 and below H5, see Fig. 3.1. Therefore, the deformation of the total system in between was measured and not the bed deformation alone.
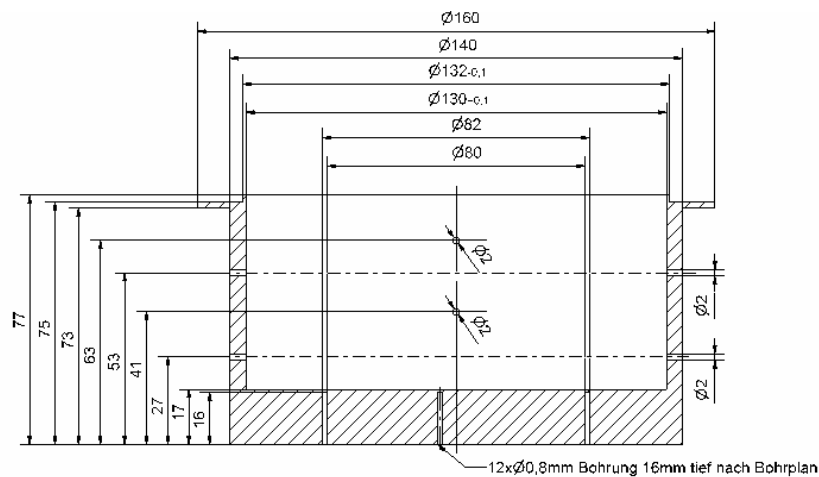

Fig. 3.3. Pebble bed container.

Figure 3.3 shows the pebble bed container in more detail. The pebble bed diameter is 130mm, the diameter of inner zone heated from below by H2 is 80mm. The position of the bores for the capillaries containing the thermocouples are also shown. The capillaries are numbered with K1, K2, K3, K4 starting from the top, see Fig. 3.2.

Figure 3.4 contains the heater plate with the heaters H2 (inner portion) and H4 (outer portion). The deep groves at D=80mm in both the heater plate and the pebble bed container, compare Figs 3.2 and 3.3, ensure that heat from H2 flows primarily vertically upward into the pebble bed; the downward flow of heat is zero because of

the temperature control. Figure 3.5 shows in more detail the arrangement of heaters H2 and H4.
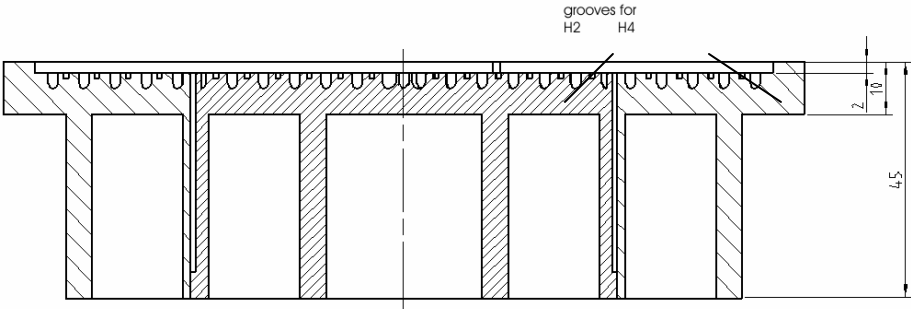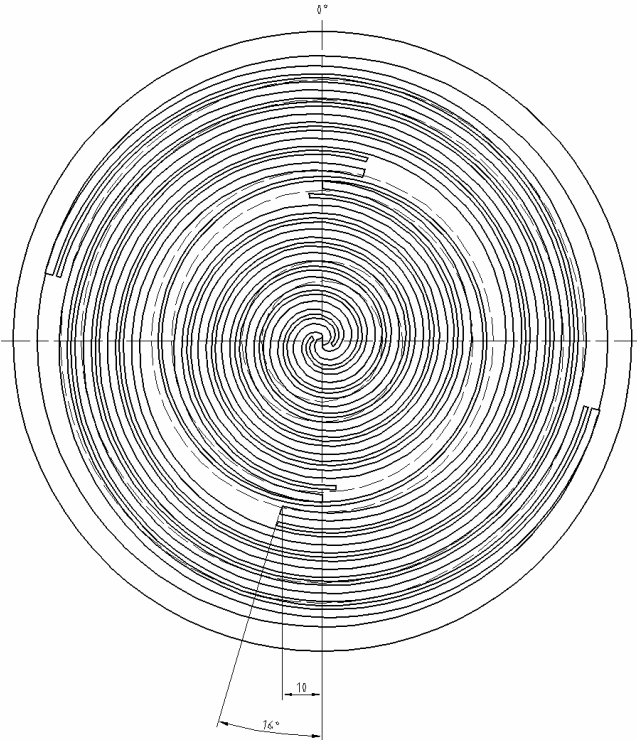

Fig. 3.4. Heater plate H2-H4.

Fig. 3.5. Arrangement of heaters H2 (inner region) and H4 (outer region) in heater plate H2-H4.

One of the rings used for the displacement measuring system is depicted in Fig. 3.6: the outer shape is dictated by space limitations (columns of the press) and the reduction of heat losses.
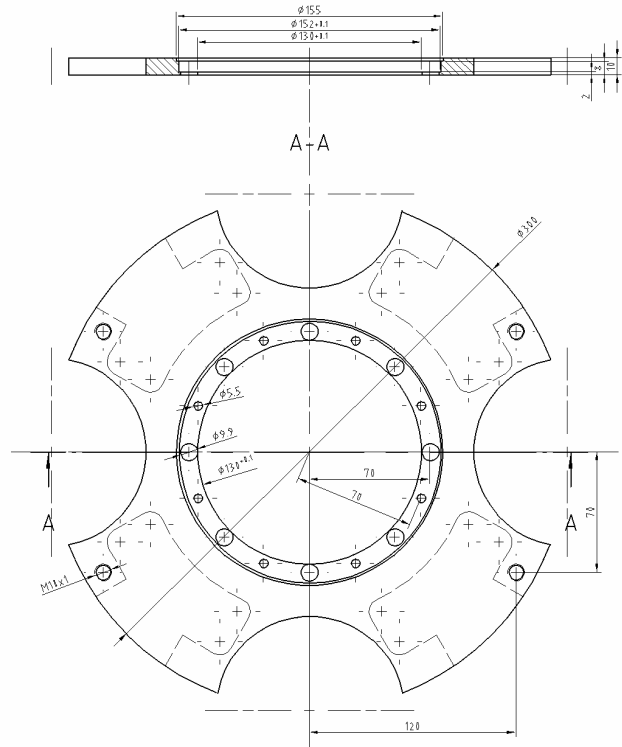
Fig. 3.6. Rings for displacement transmitters.

3.2 Theoretical determination of temperature distribution and heat losses

As outlined in Section 1, the accuracy of uniaxial arrangements is very sensitive with respect to heat losses. Besides the attempts to minimise these heat losses as much as possible by appropriate design, it is important to describe the temperature distributions in the system and to determine corresponding heat fluxes.

Temperature calculations were performed using the FLUENT code. Figure 3.7 shows the detailed 3d model of one quarter of the HECOP II geometry including the surrounding thermal insulation using in total 0.49M elements.

Figure 3.8 contains temperature distributions in a horizontal and a vertical cut. Temperatures were assumed to be constant in the plane of the heaters H2-H4 (T_{H2-H4} = 366°C) and H1-H3 (T_{H1-H3} = 336 °C). The figures show that the temperature decreases slightly radially due to heat losses through the thermal insulation. Important for the measurement accuracy is if there is a significant radial temperature decrease in the pebble bed within the diameter of 80mm above the heater H2.
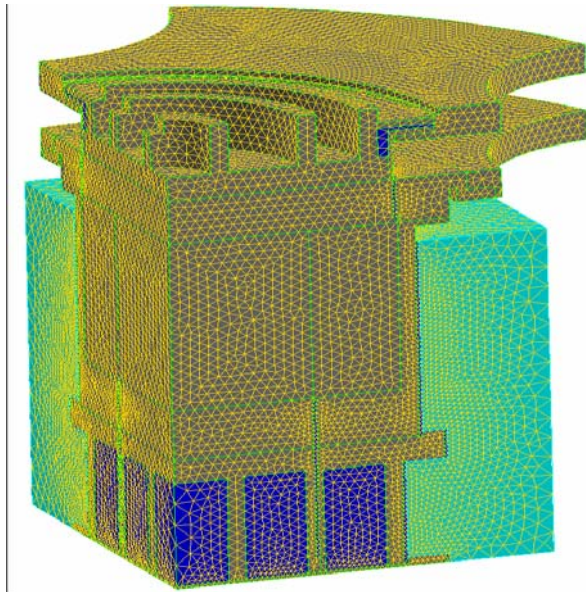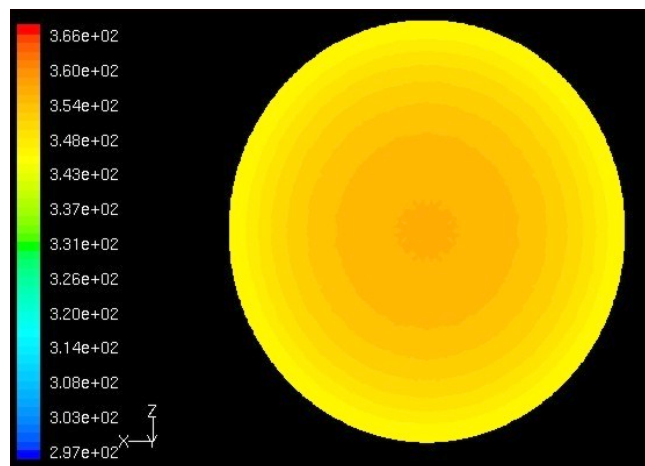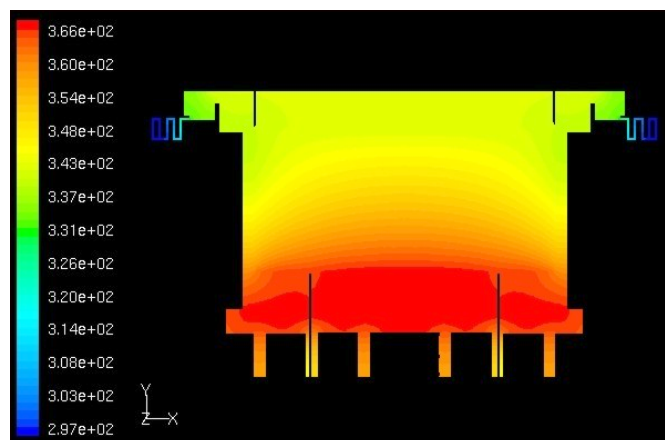
Fig. 3.7. Meshing of one quarter of HECOP II.

a) Horizontal temperature distribution in mid plane of pebble bed.

b) Vertical temperature distribution.

Fig. 3.8. Temperature distribution (T_{H2-H4} = 366°C; T_{H1-H3} = 336°C; k = 10W/(mK).

These temperature differences are more sensitively shown in the case that the temperatures in the planes H2-H4 and H1-H3 are equal. This condition is denominated with "isothermal" condition because without heat losses, no temperature differences would exist in the pebble bed. Experimentally, such "isothermal tests" were performed in order to determine heat losses, see Section 3.3.

Figure 3.9 contains radial temperature distributions at different vertical positions in the system for $T_{H2-H4} = T_{H1-H3} = 350°C$ and an assumed pebble bed conductivity of k = 10 W/(mK). Figure 3.9 shows the distributions up to a diameter of 80mm, that is, above heater H2. Of interest is the heat flowing through the cylindrical surface with D = 80mm because this heat flux represents one contribution to heat losses. In Fig. 3.9 these heat losses are about 8 Watts, however, a non-efficient thermal insulation was assumed in these calculations.
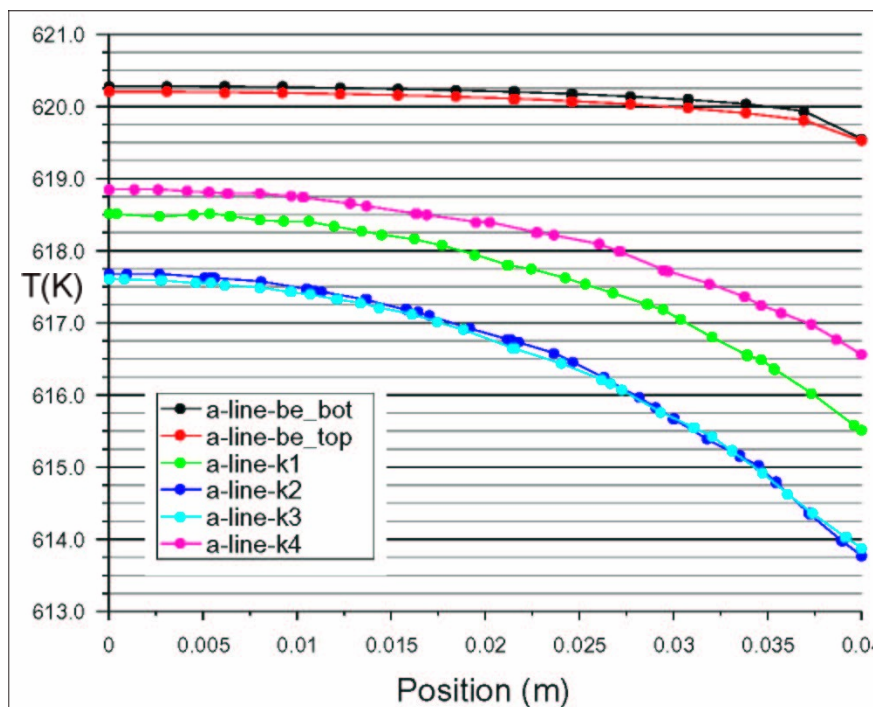

Fig. 3.9. Temperature distribution in pebble bed for $T_{H2-H4} = T_{H1-H3} = 347°C$.

Detailed sensitivity studies were performed and the dependence of the axial and radial thermal losses were determined as a function of temperature, pebble bed conductivity and thermal insulation. These calculations were very helpful for the adjustment of the guard heaters in the experiments.

3.3 Experimental procedure

Figure 3.10 shows a picture of the 1mm NGK pebbles (from [Piazza2] which had diameters between 0.8 and 1.2mm. The shape was rather spherical with some indentations on a part of the pebbles.
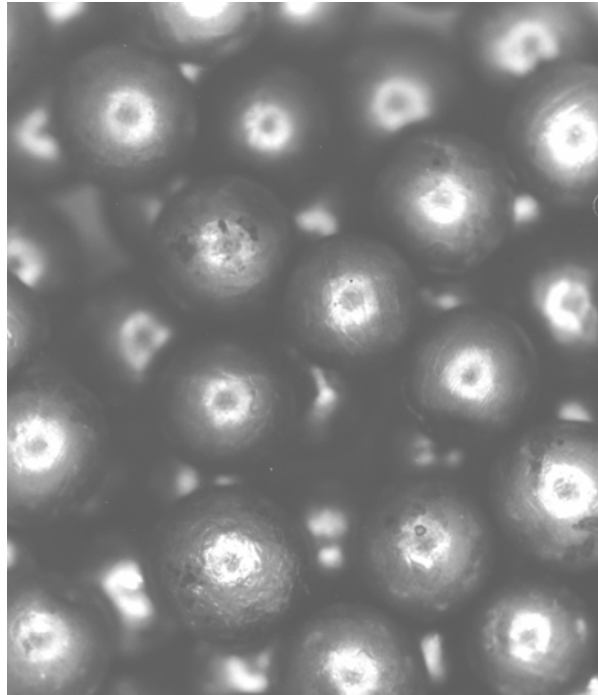

Fig. 3.10. 1mm NGK pebbles (from [11]).

The pebbles were poured outside the press into the pebble bed container and vibrated on a vibration table at 50 Hz in order to achieve dense packings. Packing factors of $\gamma \approx 63.5\%$ were achieved. These values are about 0.5% higher than obtained in previous set-ups with dense pebble beds consisting of 1mm NGK or 2mm Brush Wellman beryllium pebbles [4,8]. In the present investigations, the pebble bed has the largest diameter compared to previously used set-ups and pebble configuration disturbances due to internal thermocouples are also smaller than in most previous investigations. Additional filling experiments were performed with the 2mm beryllium pebbles, used in the previous experiments [4,8] and again packing factors of $\approx 63.5\%$ were obtained.

Therefore, $\gamma \approx 63.5\%$ appears to be relevant for the bulk density of densified pebble beds consisting of both 1mm NGK and 2mm Brush Wellman pebbles.

As the pebble bed container is connected to many thermocouple cables, a special handling arm is used for moving the pebble bed container from the vibration table into the press, for details, see [11].

After positioning the container in the press, the system was heated up at a minimum piston pressure to the desired mean bed temperature. Because of the uncertainties connected with conductivity measurements with non-deformed pebble beds, compare Section 1, conductivity measurements were performed only at p ≥ 0.3MPa.

4. RESULTS OF HECOP II

4.1 Stress-strain dependence at ambient temperature

Before starting conductivity measurements at elevated temperatures, the relationship between piston pressure (being identical to the uniaxial stress σ) and the strain ε was determined for the first pressure increase period, for ambient temperature. The results obtained shown in Fig. 4.1 agree well with previous results [8] from the HWT experiments, confirming that the new displacement measuring technique works well.
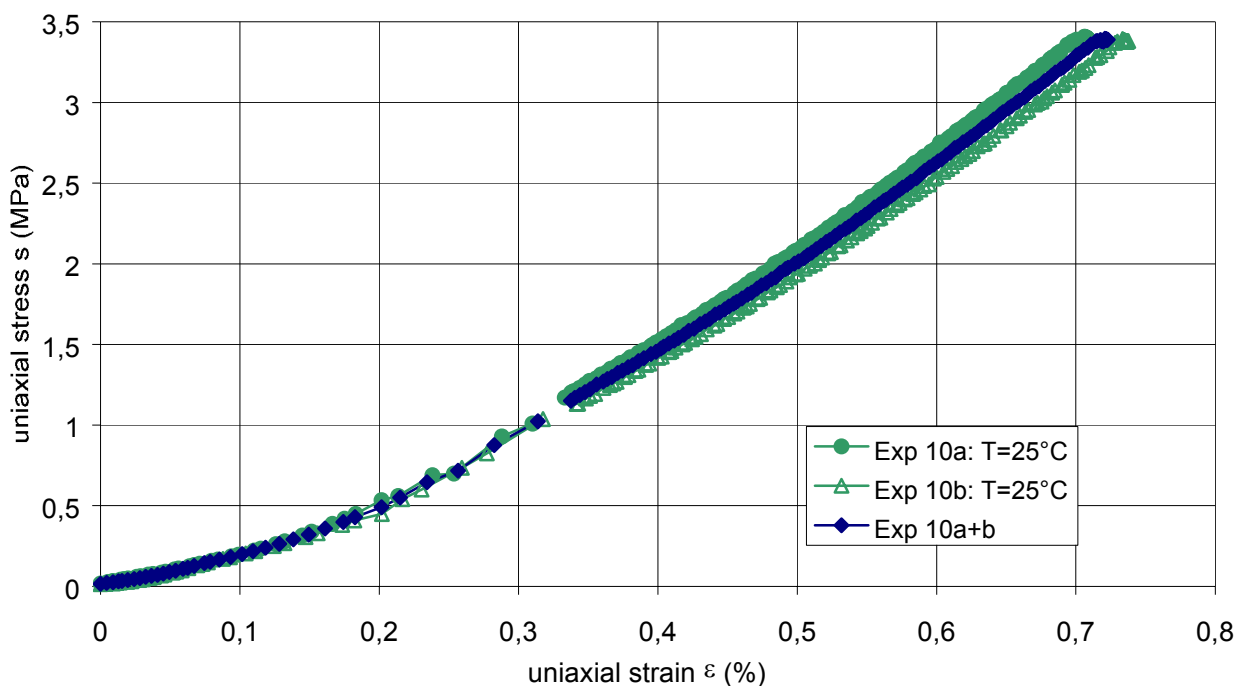

Fig. 4.1. Stress strain relationship for first pressure increase at ambient temperature.

This $\sigma-\varepsilon$ dependence for the first pressure increase can be approximated by:

$$\sigma(MPa) = 5{,}41\varepsilon(\%)^{1{,}43} \quad (4.1).$$

The $\sigma-\varepsilon$ dependence is of interest for the determination of the modulus of deformation $E(MPa) = \sigma(MPa)/\varepsilon(1)$ for the range of temperatures where no creep occurs. The following relationship is obtained:

$$E = 326\sigma^{0.3} \quad (4.2).$$

4.2 Thermal conductivity measurements at steady-state conditions

Experiments were performed with mean bed temperatures between 200 and 650°C. Whereas at temperatures of $\approx$ 200°C, creep effects are negligible; these are very pronounced at the highest temperatures. Here, a maximum bed deformation of $\varepsilon \approx 3.5\%$ was reached, a value which could not be obtained at lower temperatures without pebbles crushing because of the large pressures required, compare Eq. (4.1).
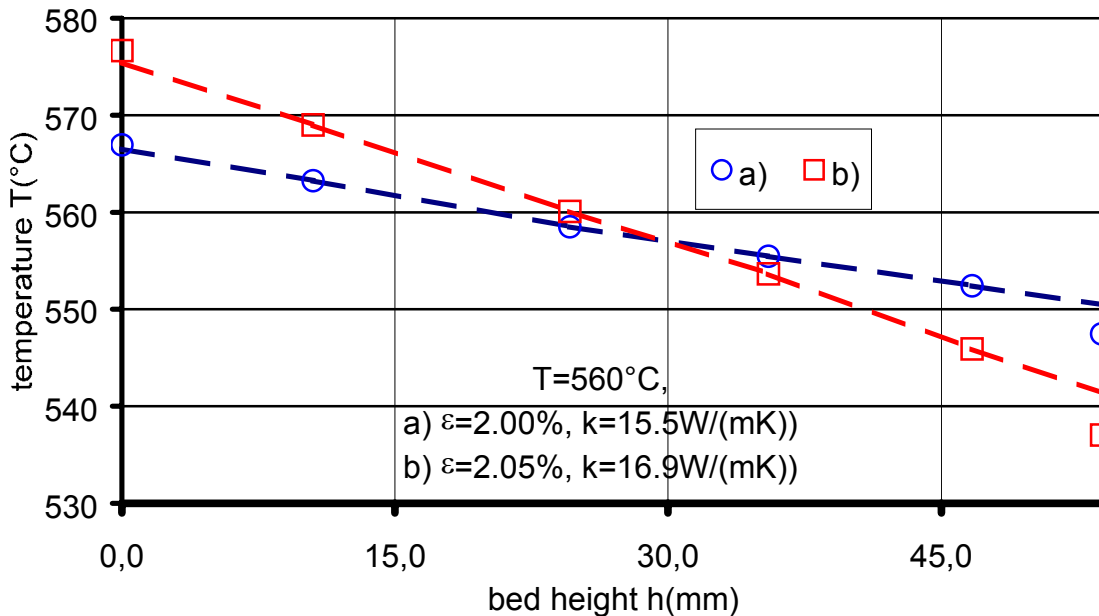

Fig. 4.2. Characteristic axial temperature distributions in the pebble bed.

When thermal creep strains occurred after the step-wise increase of the pressure level, it was waited until creep rates had become negligible before the heat transfer data were taken. In general, the conductivity k was determined using two values of pebble bed temperature differences: $\Delta T \approx 20°C$ and $\Delta T \approx 40°C$. These values are significantly smaller than used in previous experiments [5,7]; but these values were selected in order to evaluate more accurately the effect of mean bed temperature and to ensure that the bed deformation due to thermal creep strain was uniform over the bed height. In order to determine the heat losses Q_{loss}, additionally, experiments at each pressure level were performed with isothermal conditions ($\Delta T = 0°C$). These isothermal experiments were also used for the calibration of bed thermocouples with the thermocouples in the bottom and top plates which is especially important because of the small ΔT values applied.

Plotting the temperatures in the bed as a function of their axial position in the bed, a straight line is obtained indicating that the measured conductivity values are independent of the individual thermocouples and positions, as shown in Fig. 4.2.
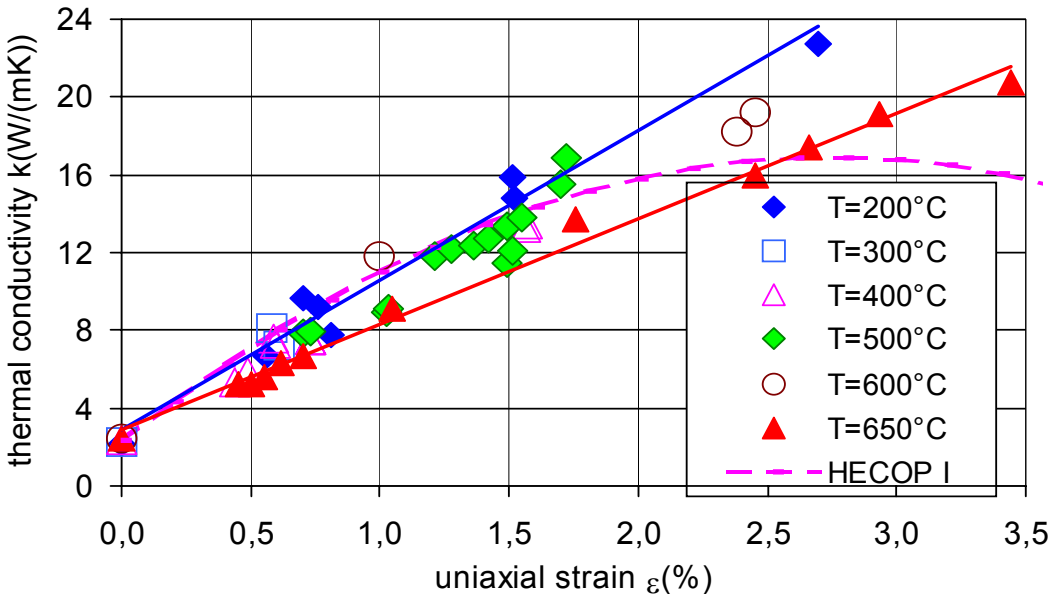

Figure 4.3. Thermal conductivity as a function of strain ε: all temperatures.

Figure 4.3 shows the summary of the results for all temperatures: As found already previously [8], a fairly linear k-ε dependence is observed for all bed temperatures T at

least up to $\varepsilon \approx 2\%$. Except for strains $\varepsilon \approx 0$, k increases with decreasing T because of the increasing beryllium conductivity, however, the temperature influence is not very strong. Pebble bed strains $\varepsilon > 0.8\%$ at T = 200°C were obtained by first performing experiments at higher temperatures and, keeping the pressure constant, cooling down to T = 200°C. Because measurements were not performed at $\varepsilon \approx 0$, the corresponding SBZ model predictions for $\varepsilon = 0\%$ are included.

4.3 Transient behaviour during the experiment at 650°C

At T=650°C, thermal creep effects are very expressed as demonstrated in Fig. 4.4 which shows the pressure p, the strain ε, the electrical power of heater H2, and the temperature difference ΔT_{cap} between the capillaries 4 and 1. This experiment lasted

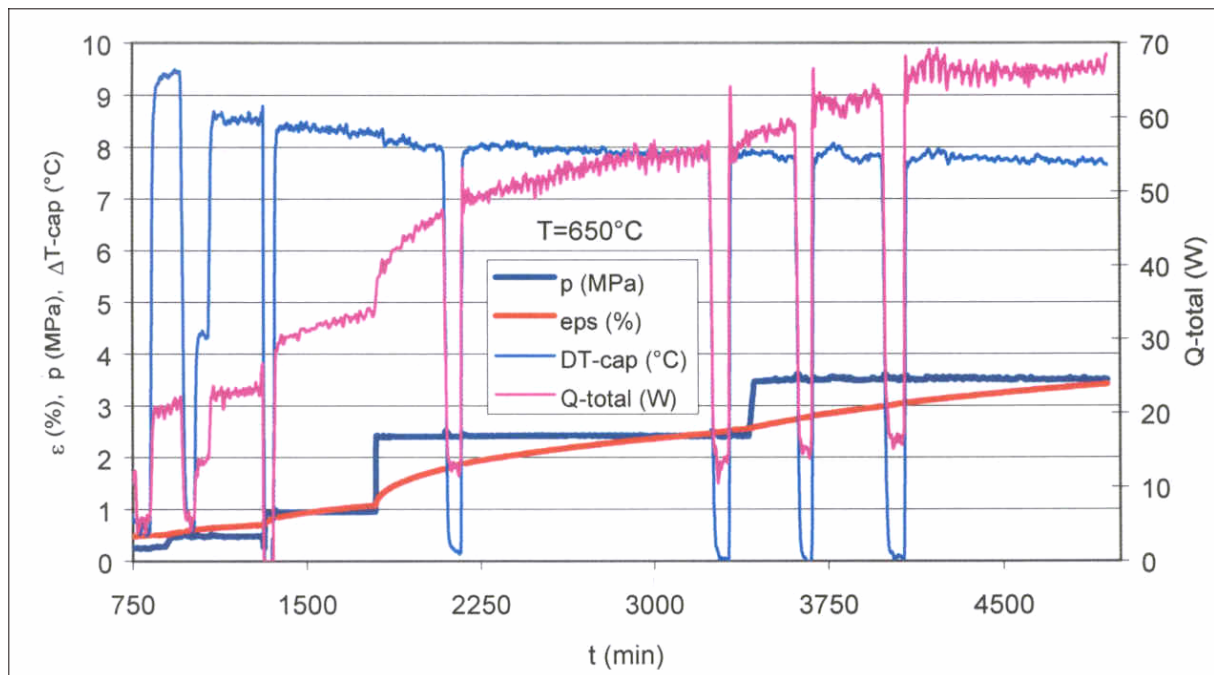Fig. 4.4. T = 650°C: measured quantities as a function of time.

several days. The pressure was imposed in several steps and all signals were continuously measured. Except for short time periods after the pressure increase, quasi-steady state conditions existed. Heat losses Q_{loss} were measured at those periods where $\Delta T_{cap} \approx 0$. In order to determine Q_{loss} for the other time periods it proved to be favourable to plot Q_{loss} as a function of k. A fairly linear relationship
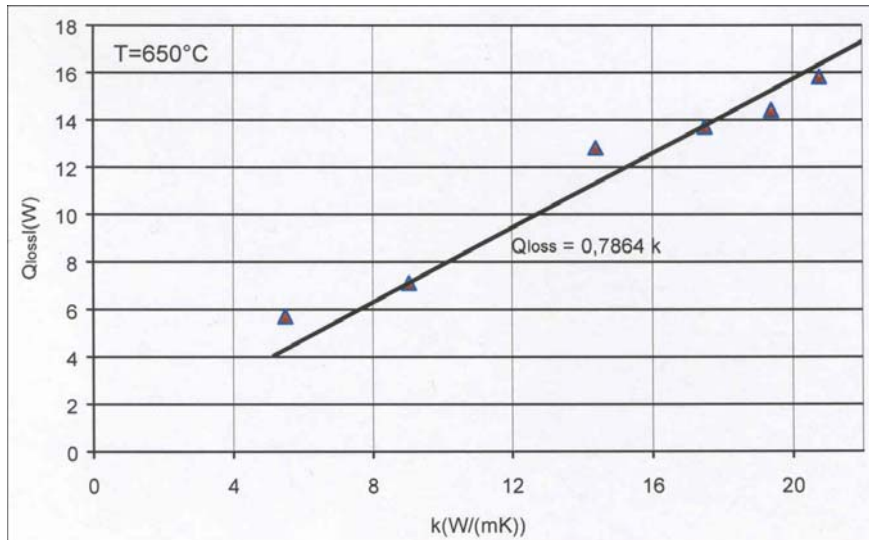
Fig. 4.5. Heat loss correlation for T = 650°C.

between Q_{loss} and k is found, see Fig.4.5. This relationship was used for the determination of k as shown in Fig. 4.6. Figure 4.7 finally shows the results for the thermal conductivity as a function of strain: the agreement with the data shown in Fig. 4.3 is very good.
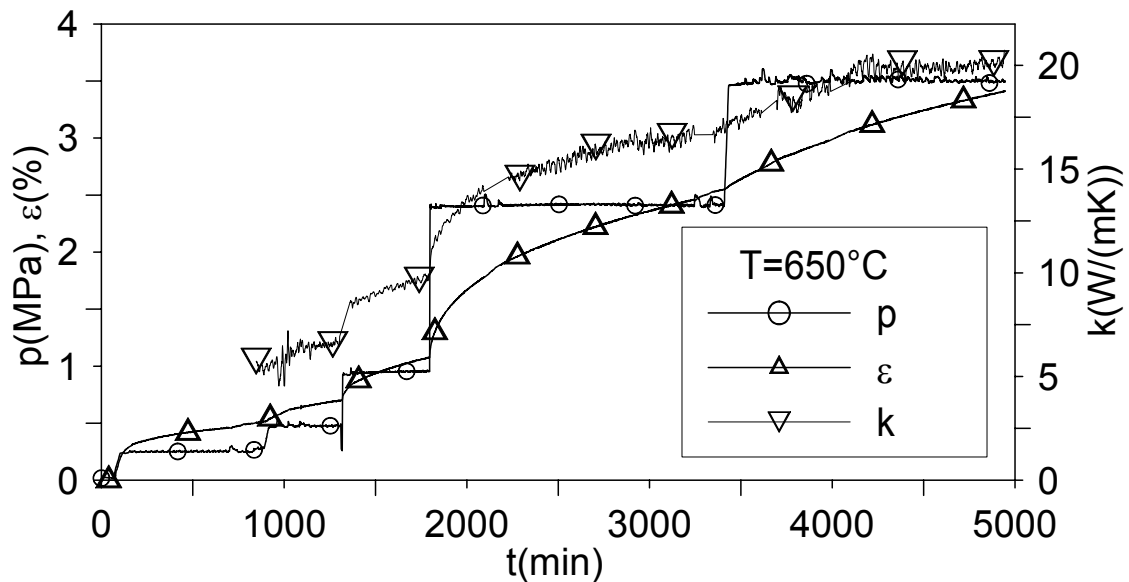

Figure 4.6 Thermal conductivity as a function of time (T = 650°C).

After cooling down of this long term experiment, the pebbles were only slightly baked together and could easily be separated. The pebbles did not show any damage.
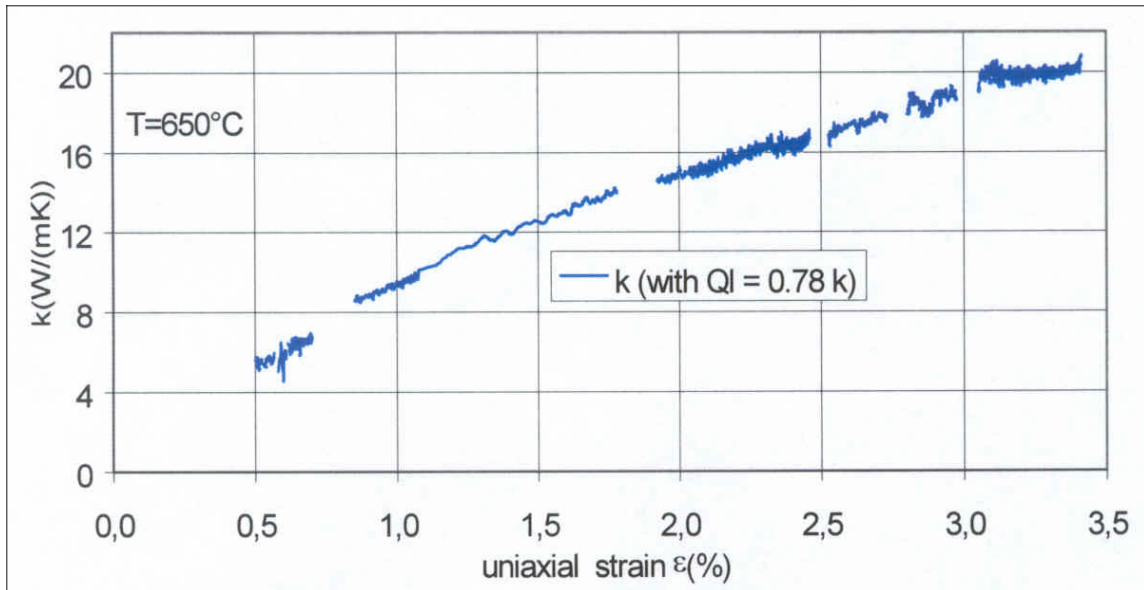
Figure 4.7 Thermal conductivity as a function of strain (T = 650°C)

Fig. 4.8. Thermal conductivity during pressure decrease for T=400°C.

4.4 Thermal conductivity during first stress decrease period and further cycles

Figure 4.8 shows results for the thermal conductivity dependence at T=400°C during pressure decrease: the changes of bed strain are very small, indicating that the pebbles are plastically deformed; in correspondence, the bed conductivity decreases

28

only slightly, except at very low pressure levels when detachments of pebble contacts are supposed to occur. In Fig. 4.8, the sequence of the experiments is also indicated. It is seen, that there is no hysteresis effect for the first pressure decrease phase and subsequent pressure increase/decrease phases.
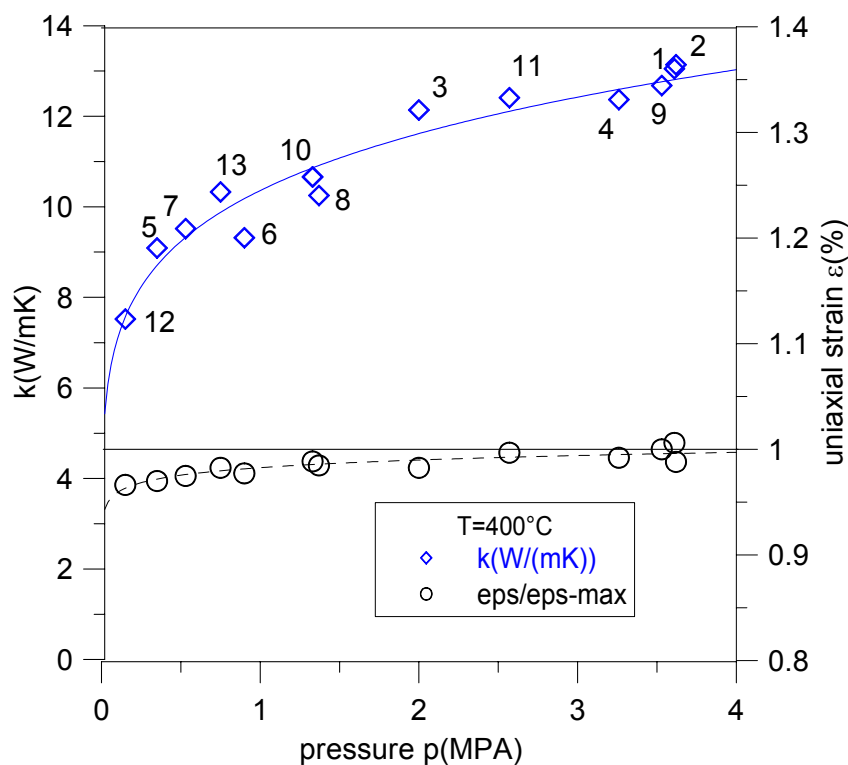

5. CORRELATIONS FOR THE THERMAL CONDUCTIVITY OF BERYLLIUM PEBBLE BEDS

5.1 Correlations for bed deformations $\varepsilon < 3.5\%$

As pointed out in Section 3, the main goal of the present investigations were measurements with deformed pebble beds. Because the measurement accuracy is lowest at $\varepsilon \approx 0$, it was not attempted to perform measurements in this range. Instead, following the procedure proposed previously [8], for non-deformed pebble beds, the SBZ model predictions are used and linear relationships are assumed between conductivity and strain. According to this procedure, the use of the normalised conductivity $k^* = (k-k_{0SBZ})/k_{0SBZ}$ is convenient. Figure 5.1 shows the corresponding results together with the values of the temperature dependent slopes B. In the non-normalised version, the correlations become

$$k = k_{0SBZ} (1 + B\varepsilon) \qquad (5.1).$$

Table 5.1 contains the values of k_{0SBZ} according to the SBZ model and the values of B for the temperatures investigated. Compared to previous HWT results [8], the present measurements are 15 - 20% higher.

Table 5.1. Temperature dependence of B.

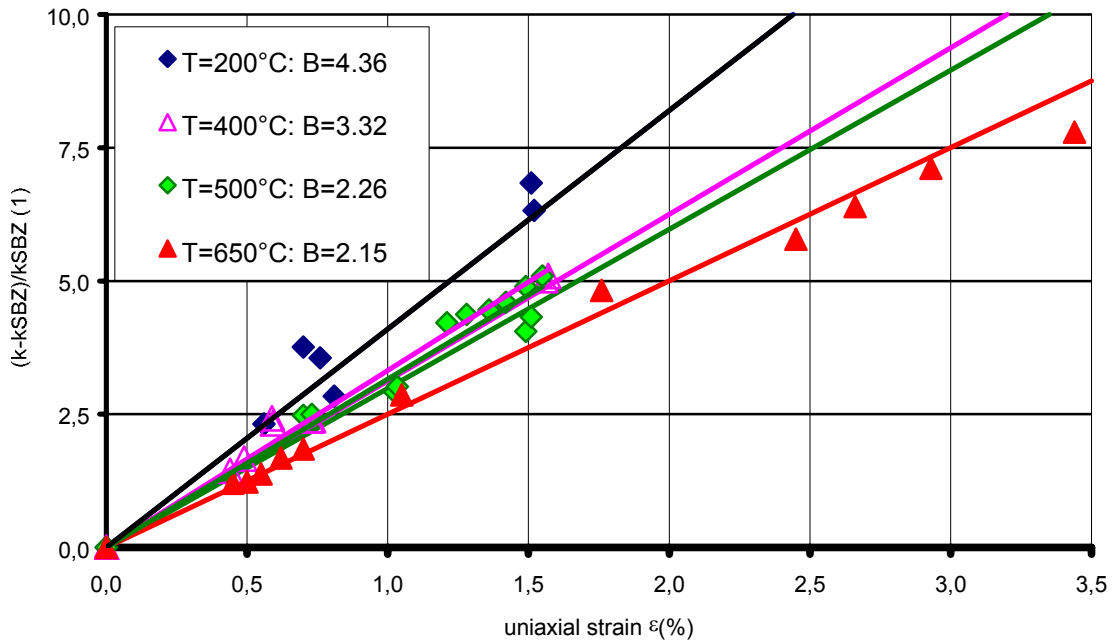| T (°C)	k_{0SBZ} (W/(mK))	B
200	2.02	4.36
400	2.20	3.32
500	2.27	2.26
650	2.36	2.15

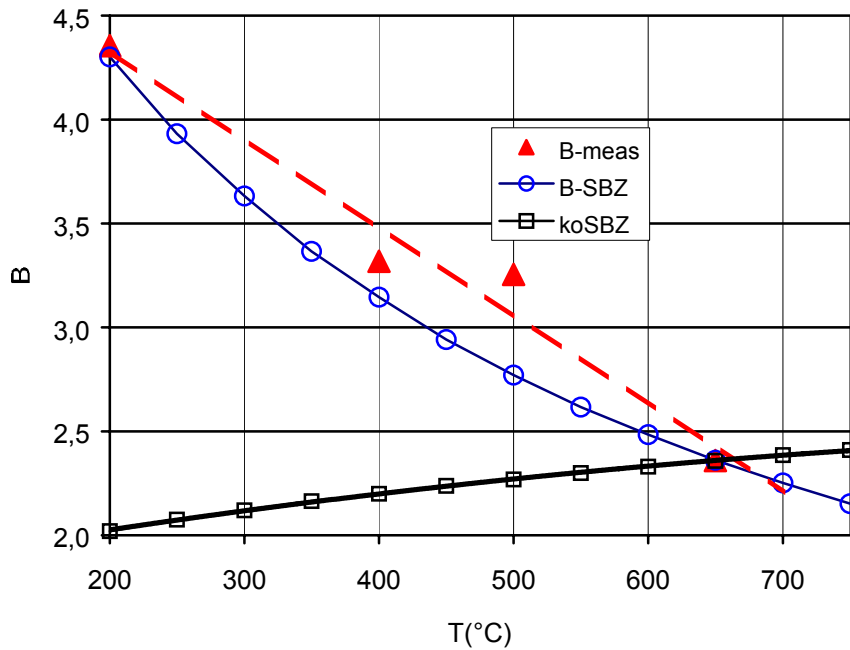Fig. 5.1. Normalised conductivity as a function of strain.

Fig. 5.2. Slopes of measured and predicted at different temperatures.

Figure 5.2 shows the slopes B of Table 5.1 as a function of temperature. The data can be fairly well fitted by the following linear relationship:

$$B = 5.18 - 0.0042 \, T(°C) \quad (5.2).$$

In order to compare the temperature dependence of the measured data with predictions from the SBZ model, the following procedure was applied: For T = 650°C and a bed deformation of 1% that value for $\rho_k{}^2$ was determined for which the SBZ model predicts the same conductivity value as measured. With this $\rho_k{}^2$ value ($\rho_k{}^2$ = 0.0063), the SBZ model conductivity values were calculated for different temperatures. Figure 5.2 shows that measured data and SBZ predictions agree quite well in the blanket relevant temperature range between 350 to 750°C. At low temperatures, the SBZ model predicts larger values than measured.

Figure 5.2 contains also SBZ conductivity values k_{0SBZ} for non-deformed beds. These values are fitted by:

$$k_{0SBZ}\,(W/(mK)) = 1.81 + 0.0012T(°C) - 5\,10^{-7}T(°C)^2 \quad (5.3)$$

With Relationships (5.2) and (5.3), the thermal conductivity of dense 1mm beryllium pebble beds is expressed by:

$$k(W/(mK)) = 1.81 + 0.0012T(°C) - 5\,10^{-7}\,T(°C)^2 + (9.03 - 1.386\,10^{-3}\,T(°C)$$
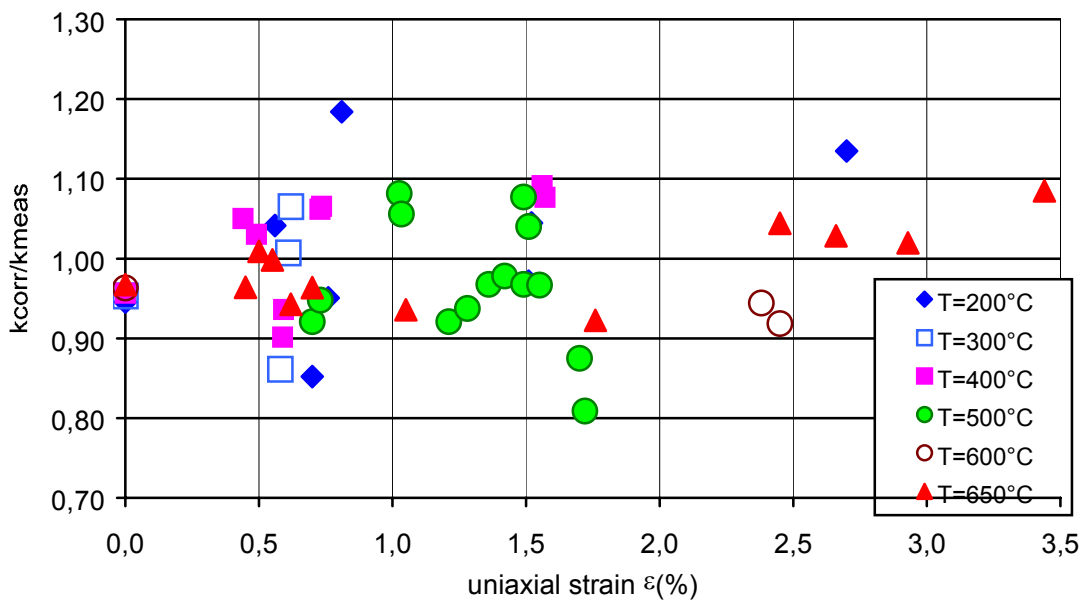$$- 7.6\,10^{-6}\,T(°C)^2 + 2.1\,10^{-9}\,T(°C)^3)\,\varepsilon(\%). \qquad (5.4).$$

Fig. 5.3. Ratio of $k_{Corr(5.4)}$ to k_{meas}.

Figure 5.3 shows the ratios of the conductivity values according Correlation (5.4) to the measured data: The mean value of all data is 0.99; the standard deviation is 0.098. At bed deformations larger than ≈ 2 %, the correlation should predict too large values because the measured data are below the linear curve, however, the deviations are mostly within the 10 % range.

Another method to establish a general correlation for deformed pebble beds is based on the idea to use generally the SBZ model in combination with an empirical relationship for the unknown contact surface ratio ρ_k^2 and the measured strain ε. In order to do this, again the ρ_k^2 values are determined in such a way that the SBZ model predicts the same values as found in the measurements.
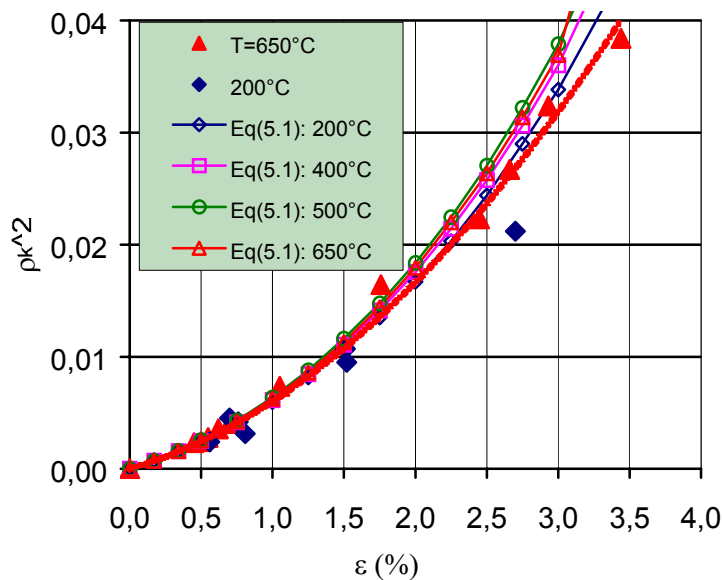

Fig. 5.4. Correlation between ρ_k^2 and measured strains ε.

Figure 5.4 shows the results for the measurements at 650 and 200°C for the total ε range. The data for 650°C are fitted by:

$$\rho_k^2 = 0.0037\varepsilon(\%) + 0.0023\ \varepsilon(\%)^2 \quad (5.5).$$

32

At very small bed deformations the slope of the curve is smaller than at large values. This can be interpreted by the fact that at the beginning of the compression, the bed is primarily compacted by pebble relocation and not by elastic/plastic deformation. The figure contains also curves determined with Eq (5.1). As expected, too large values are obtained for large bed deformations. Of interest, however, is that the temperature dependence of ρ_k^2 is very small. Therefore, Eq (5.5) is assumed to be temperature independent.
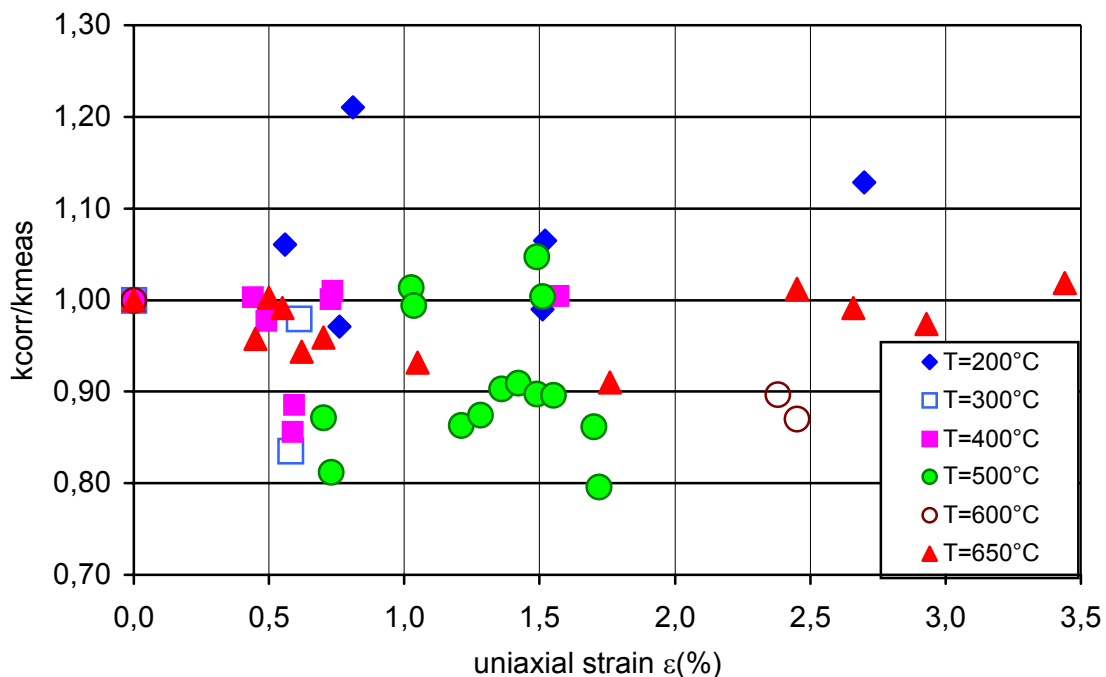
Fig. 5.5. Ratio of k_{SBZ} using Correlation (5.5) to k_{meas}.

Figure 5.5 shows the comparison between the pebble bed conductivities using the SBZ model in combination with Correlation (5.5) and the measured data: the accuracy is slightly improved at high bed compactions but in total the accuracy is not better than using directly the simple Correlation (5.4).

For fusion reactor blankets, pebble diameters different from 1mm are also envisaged. Besides, packing factors in blanket relevant geometries are not well known yet. Therefore, some considerations are outlined concerning the use of the proposed correlation for other parameter values than investigated in the present experiments:

    a) Pebble diameter d: For non-deformed pebble beds, the SBZ predicts for 2mm pebbles a conductivity which is for T=500°C ≈ 24% larger than that for 1mm

pebbles. According to the SBZ model, this difference decreases with increasing compaction, see Fig. 5.6. For a contact surface ratio $\rho_k^2 \approx 0.007$ which corresponds to a pebble bed compaction of $\varepsilon \approx 1\%$, compare Fig.5.4, the difference becomes 4%. The value $\varepsilon \approx 1\%$ might be characteristic for blankets at the begin of live. From this point of view, Correlation (5.4) is expected to predict also reasonable values for other pebble diameters.
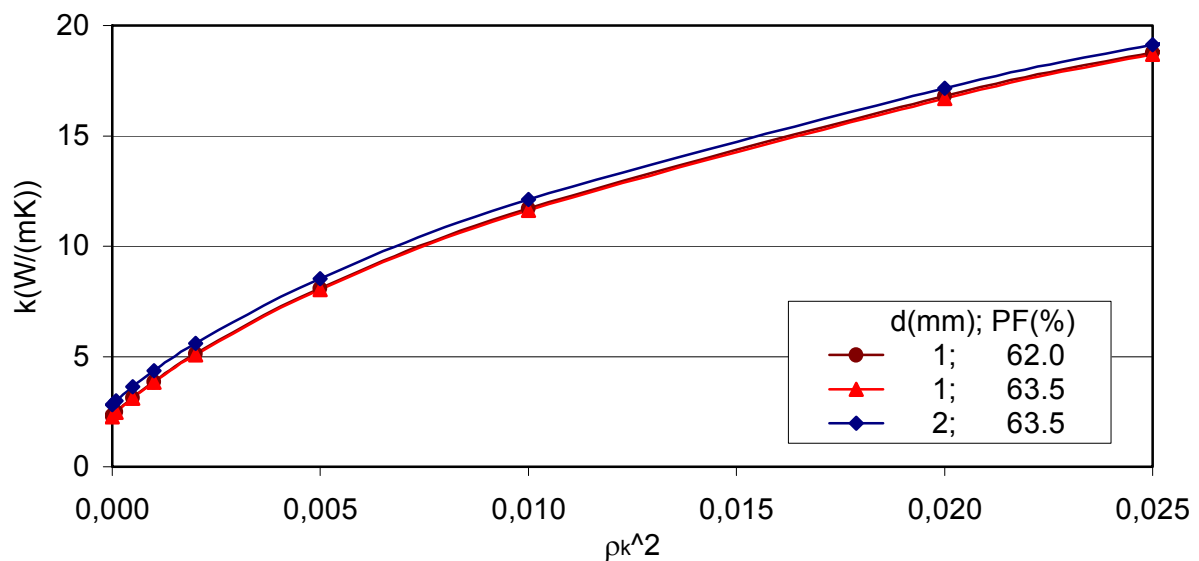

Fig. 5.6 Influence of pebble diameter and packing factor for strongly deformed pebble beds according to SBZ model.

b) Packing factor γ: It is known since long [14] that the maximum packing factor, achieved for beds densified by vibration, increases with the ratio of container diameter D to pebble diameter d and reaches a constant value for D/d > 20. The ultimate value depends on pebble shape, pebble surface and size distribution; for mono-sized spheres values of about 63% were reported [14]; different pebble diameters and deviations from sphericity can increase this value, see Section 3.3.

The reason for decreasing packing factors with decreasing container dimensions is the increasing influence of container walls: the packing factor close to walls is significantly smaller than the bulk value. Therefore, packing factors obtained for experimental set-ups might not always be relevant for the

bulk packing factor where the thermal conductivity is determined. Additionally, internal components like thermo-couple rakes represent also local disturbances, which decrease the global packing factor.

In the SBZ model the dependence of the conductivity is quite small, see Fig. 5.6. Therefore, Correlation (5.4) is expected to predict reasonable values also for other packing factors as long as densified beds are considered.

In summary, it can be concluded that the simple Correlation (5.4) is recommended to be used for dense pebble beds consisting of beryllium pebbles with diameters of 1 or 2 mm.
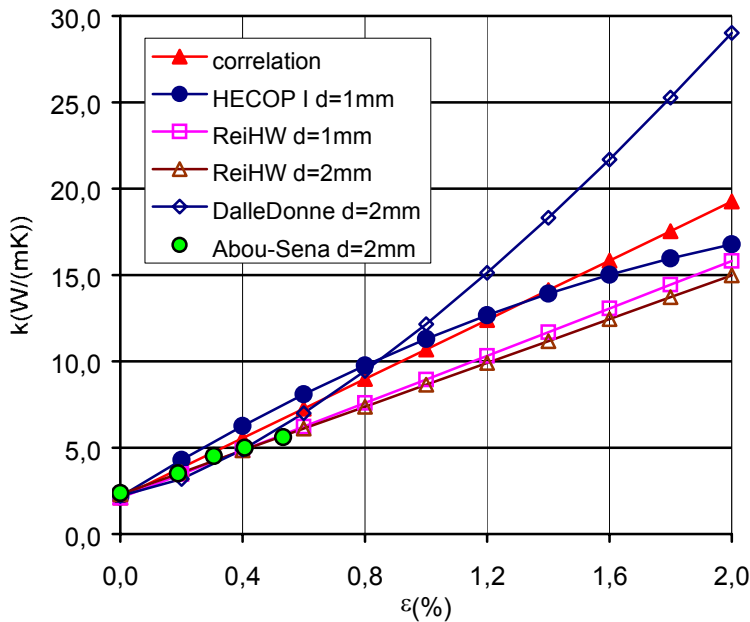

Fig. 5.7. Comparison of Correlation (5.4) with other data (T=180°C; except HECOP I: T=250°C).

Figure 5.7 contains a comparison between Correlation 5.4 and previous results for a temperature close to 200 °C: compared to the present results, the results from [8] are ≈ 20 % lower; those obtained in the first HECOP facility [11] are some percents higher in the lower strain range, however, the curve predicts increasingly lower values at bed deformations $\varepsilon > 1.5$ %. Using the conductivity-pressure correlation proposed by [4] (2mm pebbles, packing factor γ=63 %) and converting the pressure into strain by Eq. (4.1), a curve is obtained which predicts at large bed strains much too large values. Using the recent data from [7] (2 mm pebbles, packing factor

γ=60.6 %) and calculating strain again by Eq. (4.1), the experimental points are also linearly dependent on strain and agree well with the mean curve from [8]. For a packing factor of 60.6% a smaller constant than given in Eq. (4.1) should be appropriate and with this strains would become larger. This would shift the data below those from [8]. However, as discussed above, the bulk packing factor could be larger than the globally determined value.

5.2 Correlations for large bed deformations ($\varepsilon > 3,5\%$)

As outlined in Section 2.3, swelling due to irradiation might result at EOL in compactions which could be one order of magnitude large than at BOL. For sintering processes, the Correlation (2.1) was developed [17] which becomes for the packing factor $\gamma = 0.635$:

$$k/k_s = (\varepsilon/\varepsilon_{max})^{0.548} \qquad (5.6).$$

As already mentioned in Section 2, the accuracy of a correlation of the type $y = ax^b$ (with $y = k/k_s$, $x = (\varepsilon/\varepsilon_{max})$, and k_s being the conductivity of the solid material and ε_{max} is $(1-\gamma)$) predicts unsatisfactory values at small deformations. Therefore, a correlation of the type

$$y = a(x+x_0)^b - y_0 \qquad (5.7)$$

is looked for, satisfying the following conditions:
- $x = 0$: $k = k_{0SBZ}$ and slope taken from Correlation (5.1)
- $x = 1$: $k = k_s$, and slope as in Correlation (5.6).

As an example, the following relationship is obtained for 650°C with $k_s = 94$(W/mK)), relevant for non-irradiated beryllium:

$$k = 94(2.78(\varepsilon/\varepsilon_{max} + 0.22)^{0.24} - 1.92) \qquad (5.8),$$

presented in Fig. 5.8. In order to use quantitatively Eq. (5.7), the influence of irradiation on the beryllium conductivity must be known. Then, relationships similar to Eq. (5.8) can be determined.
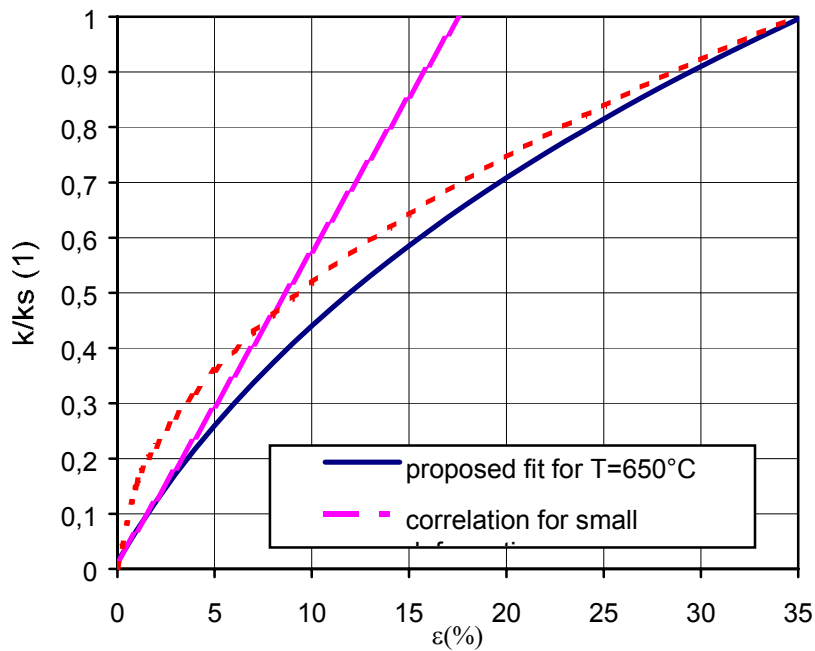

Fig. 5.8. Proposed fit for large bed deformations.

6. CONCLUSIONS

New results are presented for the thermal conductivity k of compressed beryllium pebble beds, consisting of 1mm NGK pebbles. The investigated pebble beds, are representative for dense pebble beds (achieved packing factors $\gamma \approx 63.5\%$), characteristic for bed vibration after pebble filling. Measurements were performed at bed temperatures T between 200 and 650°C and maximum pebble bed deformations up to $\varepsilon \approx 3.5\%$.

For pebble bed deformations up to $\approx 3.5\%$, two different correlations are proposed:

i) a correlation k = f(ε,T) for beryllium pebble beds, essentially based on measurements but using the conductivity values for non-deformed beryllium pebble beds predicted by the Schlünder Bauer Zehner (SBZ) model,

ii) a correlation which connects the unknown contact surface ratio of the SBZ model with the measured pebble bed deformation. In combination with this correlation, the SBZ model can be generally applied for compacted pebble beds and should be also applicable for deformed pebble beds consisting of other materials if the pebble bed deformation is known.

The overall agreement between Correlation i) and measured data is better than 10 %. It was argued that this correlation is expected predict also satisfactory values for pebble diameters different from 1mm and that the packing factor of ≈ 63.5 % is generally representative for the bulk of densified beryllium pebble beds. Therefore, Correlation i) is recommended to be used for blanket relevant densified beryllium pebble beds.

Finally, a type of correlation is presented which should be used if it shows that swelling due to irradiation effects results in much larger pebble bed deformations than presently investigated. Required, however, is the knowledge of the dependence of the beryllium conductivity on neutron fluence.

With the present data on thermal conductivity of deformed beryllium pebble beds, the corresponding data on thermal creep [9], also obtained in the HECOP II facility, and the already existing data for ceramic breeder pebble beds [2], a complete set of pebble bed data exists now, relevant for the beginning of reactor life where irradiation effects are still negligible. These data are required as input for codes to determine the thermal-mechanical interaction between the pebble beds and the blanket structure.

ACKNOWLEDGEMENTS

REFERENCES

[1]   S. Hermsmeyer, B. Dolensky, J. Fiek, U. Fischer, C. Köhly, S. Malang, P. Pereslavtsev, J. Rey, Z. Xu, Revision of the EU Helium cooled pebble bed blanket for DEMO, 20th SOFE, San Diego, USA, Oct. 14-17, 2003, Piscataway, N.J. : IEEE, 2003 pp. 440-445, ISBN 0-7803-7908-X

[2]   J. Reimann, L. Boccaccini, M. Enoeda, A. Y. Ying, Thermomechanics of solid breeder and Be pebble bed materials, ISFNT-6, San Diego, USA, April 7-12, 2002, Fusion Engineering and Design, 61-62 (2002) pp. 319-331.

[3]   M. Enoeda, K. Furuya, H. Takatsu, S. Kikuchi, T. Hatano, Effective thermal conductivity measurements of the binary pebble beds by hot wire method for the breeding blanket, Fusion Technology, Vol. 34, No. 3, Pt. 2, Nov. 1998, pp. 877-881.

[4]   M. Dalle Donne, A. Goraieb, G. Piazza, F. Scaffidi-Argentina, Experimental investigations on the thermal and mechanical behaviour of single size beryllium pebble beds, Fusion Technology, Vol. 38, No. 3, Nov. 2000, pp. 290-298.

[5]   M. Dalle Donne, G. Sordon, Heat transfer in pebble beds for fusion blankets, Fusion Technology 17, July 1990, pp.597-635.

[6]   F. Tehranian and M. Abdou, Experimental study of the effect of external pressure on particle bed effective thermal properties, Fusion Techn. Vol. 27, May 1995, pp. 298-313.

[7]   A. Abou-Sena, A. Ying, M. Abdou, Experimental investigation and analysis of the effective thermal properites of beryllium packed beds, Fusion Science and Technology, Vol. 44, July 2003, pp. 79-84.

[8]   J. Reimann, S. Hermsmeyer, G. Piazza, G. Wörner, Thermal conductivity measurements of deformed beryllium pebble beds by hot wire method, CBBI-9, Toki, Japan, Sept. 27-29, 2000, Tokyo : Univ. of Tokyo, 2002, pp. 199-214.

[9]   J. Reimann, H. Harsch, Thermal creep of beryllium pebble beds, 23rd SOFT, 20-24 Sept., Venice, Italy, 2004.

[10]   J. Reimann; S. Hermsmeyer, Thermal Conductivity of Compressed Ceramic Breeder Pebble Beds, ISFNT-6, San Diego, USA, April 7-12, 2002, Fusion Engineering and Design, 61-62 (2002) pp. 345-351.

[11] G. Piazza, J. Reimann, G. Hofmann, S. Malang, A. Goraieb, H. Harsch, Heat transfer in compressed beryllium pebble beds, 22nd Symp Fusion Technology, Helsinki, Finland, September, 9-13, 2002, Fusion Engineering and Design, 69 (2003) pp. 227-231.

[12] E. V. Schlünder, Particle heat transfer, Proc 7th Int. Heat Transfer Conf., München, Germany, September 6-10, 1982, Hemisphere Publ. Co. Vol. 1, RK10, 195-212, 1982.

[13] VDI-Wärmeatlas, Section Dee, Springer Verlag, 9.Auflage 2002.

[14] R. K. McGeary, Mechanical packing of spherical particles, J. Am. Ceram. Soc., 44, 10, 513, 1961.

[15] J. Reimann, R. A. Pieritz, M. di Michiel, C. Ferrero; Inner structures of compressed pebble beds determined by X-ray tomography, 23rd Symposium Fusion Technology, Venice, Italy, 20-24 Sept., 2004.

[16] J. Reimann, G. Piazza, H. Harsch; Thermal conductivity of compressed beryllium pebble beds, Tokyo, Japan, May 22-27, 2005.

[17] C. Argento, D. Bouvard, Modeling the effective thermal conductivity of random packing of spheres through densification; Int. J. Heat Mass. Transfer, Vol. 39, No. 7, pp.1343-1350, 1996.